Systematic Entomology

Systematic Entomology (2014), DOI: 10.1111/syen.12078

Systematics and evolution of gall formation in the plant-associated genera of the wasp subfamily Doryctinae (Hymenoptera: Braconidae)

ALEJANDRO ZALDÍVAR-RIVERÓN[1], JUAN J. MARTÍNEZ[2], SERGEY A. BELOKOBYLSKIJ[3], CARLOS PEDRAZA-LARA[1], SCOTT R. SHAW[4], PAUL E. HANSON[5] and FERNANDO VARELA-HERNÁNDEZ[1]

[1]Colección Nacional de Insectos, Instituto de Biología, Universidad Nacional Autónoma de México, Coyoacán, México, [2]División Entomología, Museo Argentino de Ciencias Naturales 'Bernardino Rivadavia', CONICET, Buenos Aires, Argentina, [3]Museum and Institute of Zoology, Polish Academy of Sciences, Warsaw, Poland, [4]Department of Ecosystem Science and Management (3354), University of Wyoming, Laramie, WY, U.S.A. and [5]Escuela de Biología, Universidad de Costa Rica, San Pedro de Montes de Oca, Costa Rica

Abstract. Gall formation is a specialised form of phytophagy that consists of abnormal growth of host plant tissue induced by other organisms, principally insects and mites. In the mainly parasitoid wasp subfamily Doryctinae, gall association, represented by gall inducers, inquilines and their parasitoids, is known for species of seven genera. Previous molecular studies recovered few species of six of these genera as monophyletic despite their disparate morphologies. Here, we reconstructed the evolutionary relationships among 47 species belonging to six gall-associated doryctine genera based on two mitochondrial and two nuclear gene markers. Most of the Bayesian analyses, performed with different levels of incomplete taxa and characters, supported the monophyly of gall-associated doryctines, with *Heterospilus* (Heterospilini) as sister group. *Percnobracon* Kieffer and Jörgensen and *Monitoriella* Hedqvist were consistently recovered as monophyletic, and the validity of the monotypic *Mononeuron* was confirmed with respect to *Allorhogas* Gahan. A nonmonophyletic *Allorhogas* was recovered, although without significant support. The relationships obtained and the gathered morphological and biological information led us to erect three new genera originally assigned to *Psenobolus*: *Ficobolus* **gen.n.** (*F. paniaguai* **sp.n.** and *F. jaliscoi* **sp.n.**), *Plesiopsenobolus* **gen.n.** (*Pl. mesoamericanus* **sp.n.**, *Pl. plesiomorphus* van Achterberg and Marsh **comb.n.**, and *Pl. tico* **sp.n.**), and *Sabinita* **gen.n.** (*S. mexicana* **sp.n.**). The origin of the gall-associated doryctine clade was estimated to have occurred during the middle Miocene to early Oligocene, 16.33–30.55 Ma. Our results support the origin of true gall induction in the Doryctinae from parasitoidism of other gall-forming insects. Moreover, adaptations to attack different gall-forming taxa on various unrelated plant families probably triggered species diversification in the main *Allorhogas* clade and may also have promoted the independent origin of gall formation on at least three plant groups. Species diversification in the remaining doryctine taxa was probably a result of host shifts within a particular plant taxon and shifts to different plant organs.

This published work has been registered in ZooBank, http://zoobank.org/urn:lsid:zoobank.org:pub:0021F253-4ABA-4EAA-A7A9-FC0AD1932EA3

Correspondence: Alejandro: Zaldívar-Riverón, Colección Nacional de Insectos, Instituto de Biología, Universidad Nacional Autónoma de México, 3er. circuito exterior s/n, Cd. Universitaria, Copilco, Coyoacán, C. P. 04510, D. F., México. E-mail: azaldivar@ib.unam.mx

[Version of Record, published online 26 May 2014]

Introduction

Gall formation is a highly developed form of phytophagy that consists of abnormal growth of plant tissue induced by adult, larval or other immature stages of species of various insect and mite orders (Raman *et al.*, 2005). Gall formation is triggered by a chemical stimulus induced by the adult arthropod when it oviposits and/or by its offspring during feeding, which isolates meristematic cells of the host plant from their normal course of differentiation, and from which the latter feed and shelter until they complete their development (Doss *et al.*, 2000; Harper *et al.*, 2004; Csóka *et al.*, 2005). This has been recorded to occur in a number of vascular plant families, with most gall inducers being highly specific both to the host plant species and to the plant parts (leaves, stems, roots) that they attack (Raman *et al.*, 2005). The ecological role of gall-inducing species is significant because they can, for example, affect plant productivity by reducing the rate of photosynthesis in leaves (Larson, 1998; Patankar *et al.*, 2011), the amino acid content in phloem sap (Koyama *et al.*, 2004) or the levels of nutrients and secondary compounds (Hartley, 1998).

In Hymenoptera, gall formation is mostly known in the Cynipidae, where it is the predominant biology for most species (Csóka *et al.*, 2005). Gall formation also occurs in some sawflies (Roininen *et al.*, 2005; Taeger *et al.*, 2010), several members of Chalcidoidea (LaSalle, 2005) and Braconidae (Wharton & Hanson, 2005). In the mainly parasitoid family Braconidae, phytophagy has evolved independently in three subfamilies: Mesostoinae, Braconinae and Doryctinae (Zaldívar-Riverón *et al.*, 2006). Currently, only few braconid species have been confirmed to be phytophagous, with most of them being gall inducers (Braconinae: Flores *et al.*, 2005; Perioto *et al.*, 2011; Doryctinae: see below; Mesostoinae: Dangerfield & Austin, 1998). However, several other members of Braconinae, Mesostoinae and Doryctinae have also been associated with galls, with some of them being inquilines (i.e. suspected to feed on galls made by other gall-inducing insects) or parasitoids (van Achterberg & Weiblen, 2000; Wharton & Hanson, 2005; Wei *et al.*, 2013).

Gall association in the Doryctinae has been reported for species of seven genera (Wharton & Hanson, 2005) on 12 vascular plant families (Fig. 1A-F; Table S1): *Allorhogas* Gahan, *Donquickeia* Marsh, *Labania* Hedqvist, *Monitoriella* Hedqvist, *Mononeuron* Fischer, *Percnobracon* Kieffer and Jörgensen, and *Psenobolus* Reinhard. Members of these genera are restricted to the Neotropics except one species of *Allorhogas*, *A. semitemporalis* Fischer, which was described from Iraq (Fischer, 1960), although the collecting locality of the type specimens needs confirmation. Gall formation has so far been confirmed in only a few species of *Allorhogas* and one of *Monitoriella* (de Macêdo & Monteiro, 1989; Infante *et al.*, 1995). Field observations, however, suggest that this might be the predominant biology within the latter two genera and within *Labania*, *Mononeuron* and *Psenobolus* (Marsh, 2002; Nunes *et al.*, 2012; P.E. Hanson, unpublished data).

Allorhogas is by far the most speciose gall-associated doryctine genus with 45 described and a large number of undescribed species; it is also the genus with the most host plant family records and is suspected to contain both gall inducer and parasitoid (or inquiline) species. The remaining genera, however, appear to have lower species richness and more restricted host plant family ranges (Table S1). Species of *Monitoriella* (nine described species) apparently are only associated with galls on Araceae, whereas *Labania* and *Psenobolus* (4 and 11 spp., respectively) appear to be exclusively associated with galls on *Ficus* species (Moraceae). The monotypic *Mononeuron* and the two described species of *Donquickeia* have been reported from galls on species of Annonaceae and Asteraceae and Myrtaceae, respectively, whereas records for *Percnobracon* (five described species) are all from Fabaceae. Due to their considerably different external morphologies, the gall-associated genera were originally placed in distinct tribes and even subfamilies (Shenefelt & Marsh, 1976; Belokobylskij, 1992; Marsh, 1997b). Nevertheless, two recent molecular phylogenetic studies including a few species from five of these genera (except *Donquickeia* and *Mononeuron*) consistently recovered them within a single clade, thus revealing a single origin of this biology in the subfamily (Zaldívar-Riverón *et al.*, 2007, 2008).

Despite the above molecular phylogenetic studies, the relationships of the gall-associated doryctines within the subfamily and the monophyly of most of their genera are still unclear. Previous authors have reported considerable variation in various key external morphological features among species of *Allorhogas*, suggesting that this taxon could be nonmonophyletic (Marsh, 1993; Martínez *et al.*, 2008; Martínez & Zaldívar-Riverón, 2013). Moreover, species of *Mononeuron* and *Donquickeia* share various similar external morphological features with members of *Allorhogas* (Fischer, 1981; Marsh, 1993; Nunes *et al.*, 2012). In addition, recent collections of species assigned to *Psenobolus* have shown not only significant variation in their external morphological features, but also in the plant parts that they attack.

Here, we reconstructed the phylogenetic relationships amongst 47 species belonging to six of the seven known gall-associated doryctine genera using two nuclear and two mitochondrial (mt) gene markers. The monophyly of this group, and the limits of each genus, were assessed based on the relationships recovered, and taxonomic inferences were also made based on the morphological congruence among the taxa involved. Moreover, the times of origin and diversification of the gall-associated doryctines were estimated using a Bayesian relaxed molecular clock method in order to infer the evolution of host plant association in the group.

Methods

Taxon sampling

Forty-seven species assigned to six gall-associated doryctine genera were included: *Allorhogas* (30 spp.), *Labania* (1 sp.), *Mononeuron* (1 sp.), *Monitoriella* (3 spp.), *Percnobracon* (4 spp.) and *Psenobolus* (8 spp.). The species examined covered

most of the known morphological variation and geographic distribution of each genus.

Fourteen species belonging to nine doryctine genera were employed in the phylogenetic analyses to test the monophyly of the gall-associated group. Records for species of these genera whose biology is known indicate that all are parasitoids and they are not associated with galls. These included the following seven genera that were previously recovered within a major South American doryctine clade (Zaldívar-Riverón *et al.*, 2007, 2008): *Aivalykus* Marsh (1 sp.), *Ecphylus* Foerster (2 spp.), *Hecabolus* Curtis (1 sp.), *Heterospilus* Haliday (4 spp.), *Notiospathius* Matthews and Marsh (1 sp.), *Tarasco* Marsh (1 sp.) and *Trigonophasmus* Enderlein (1 sp.). Two species belonging to an undescribed doryctine genus morphologically similar to *Notiospathius* were also included. This new genus appeared closely related to a *Heterospilus* + gall-associated clade in a recent molecular phylogenetic study (Ceccarelli & Zaldívar-Riverón, 2013). Moreover, sequences of two Australian species of *Ontsira* were merged into a single terminal taxon and selected to root all the trees. The Australian species of *Ontsira* belong to an Australian doryctine clade, which was sister to the South American one (Zaldívar-Riverón *et al.*, 2008). Five of the above outgroup taxa were each represented by sequences of two different species. A list of the specimens included in the molecular phylogenetic analyses, their localities and GenBank accession numbers for the four examined loci are given in Table S2.

Laboratory protocols

DNA sequences of two mt and two nuclear gene fragments were examined: ~650 bp of the cytochrome oxidase I (*COI*) and ~350 bp of the ribosomal (r) *16S* mtDNA genes, and ~700 bp of the second and third domain regions of the r *28S* and 473 bp of the *wingless* (*wg*) nuclear genes. These four gene fragments have been widely employed in molecular phylogenetic analyses of a number of braconid taxa, where they have been shown to be useful at different taxonomic levels (e.g. Dowton & Austin, 2001; Zaldívar-Riverón *et al.*, 2008; Ceccarelli & Zaldívar-Riverón, 2013).

Genomic DNA extraction was carried out with the DNeasy blood and tissue extraction kit (Qiagen, Valencia, CA, USA) using the nondestructive technique described in Ceccarelli *et al.* (2012). Amplifications of the four gene fragments were carried out using a total volume of 12.5 μL, with 1× PCR buffer, 0.5 mM of each primer, 0.2 mM of each dNTP, 2 mM $MgCl_2$, 1 U of platinum Taq polymerase (Invitrogen), 5 μL of template DNA (about 10–50 ng) and 4.97 μL of ddH2O. A list with the primers and the annealing temperatures employed for the PCRs performed are given in Table S3. The complete PCR programs for the gene markers amplified are those followed by Ceccarelli *et al.* (2012) for *COI*, *28S* and *wg*, and Dowton & Austin (2001) for *16S*. Unpurified PCR products were sent for DNA sequencing to the High-Throughput Genomics Unit at the University of Washington (http://www.htseq.org/index.html).

Sequences were edited with Sequencher 4.1.4 (Gene Codes Corp.). *COI* and *wg* sequences were manually aligned according to their translated amino acids with MacClade v4.06 (Maddison & Maddison, 2000), whereas *28S* and *16S* sequences were aligned based on their secondary structure, which were modelled using the program Mxscarna (http://mxscarna.ncrna.org/). These models helped to detect ambiguously aligned loop regions, which were excised from the *16S* dataset. For the *28S*, ambiguously aligned loop regions were initially excised, and those groups of sequences with conserved length for each of these regions were subsequently included in blocks at the end of the alignment following the approach described by Zaldívar-Riverón *et al.* (2006). A file containing the concatenated matrix with all examined taxa and sequences is provided in File S1.

Phylogenetic analyses

DNA sequences of the four gene markers examined could not be generated for all terminal taxa. We therefore carried out analyses using the following five datasets to evaluate the effect of missing taxa and characters in our phylogenetic reconstruction: (i) all available taxa and sequences (*all*); (ii) only taxa with sequences generated for the four gene fragments (*four genes*); (iii) only taxa with sequences generated for at least two gene fragments (*two genes*); (iv) only taxa with sequences generated for at least three gene fragments (*three genes*); and (v) all taxa, excluding *16S* (*N16S*). The latter dataset was analysed because terminal taxa were highly incomplete for the *16S* partition. Moreover, the alignment of this gene fragment resulted in the excision of 125 nucleotide positions, which were contained in five ambiguously aligned loop regions.

Partitioned Bayesian and maximum likelihood (ML) analyses were carried out for each dataset using MrBayes v3.2.2 (Ronquist *et al.*, 2012) and RAxML v7.2.8 (Stamatakis *et al.*, 2008), respectively. Bayesian analyses consisted of two simultaneous runs of 20 million generations each, and used default priors and sampling trees every 1000 generations. *COI* and *wg* were partitioned according to their codon positions, whereas *28S* and *16S* were divided into two partitions, one for the stem and one for the unambiguously aligned loop regions. All partitions employed the GTR + G evolutionary model (Lanave *et al.*, 1984) for the ML analyses. Evolutionary models for the ten different partitions (Table S4) were selected for the Bayesian analyses according to the Akaike information criterion implemented in MrModeltest v2.3 (Nylander, 2004). Stationarity in all analyses occurred before 1 million generations, although their burn-ins were set at 10 million generations to ensure convergence of the standard deviation of split frequencies. ML analyses were executed using 200 ML tree searches with a random starting tree and 200 ML tree searches that started from a bootstrapped tree topology. Nodal support was estimated using 1000 bootstrap replicates.

Test of alternative hypotheses

Our best estimate of phylogeny recovered from the Bayesian analyses was tested against the following three alternative

hypotheses involving three morphologically heterogeneous genera: (i) species assigned to *Allorhogas* as monophyletic; (ii) *Allorhogas* + *Mononeuron* as monophyletic; and (iii) species assigned to *Psenobolus* as monophyletic.

Our preferred Bayesian phylogeny was tested against the alternative hypotheses with Bayes factors comparisons, which were calculated from estimates of marginal likelihoods using the stepping stone (SS) sampling approach (Xie *et al.*, 2011) in MrBayes. The parameters employed for these tests are the same as those described in Ceccarelli & Zaldívar-Riverón (2013). Our best estimate of phylogeny derived from the ML analyses was tested with the three alternative hypotheses using Shimodaira-Hasegawa (SH; Shimodaira & Hasegawa, 1999) and Approximate Unbiased (AU; Shimodaira, 2002) tests with 50 000 RELL bootstrap replicates in the program TreeFinder (Jobb *et al.*, 2004).

Divergence-time estimates

We investigated the origin and diversification of the gall-associated doryctines using a Bayesian relaxed molecular clock analysis with BEAST v1.7.4 (Drummond *et al.*, 2012). This analysis was performed with the *all* dataset for 20 million generations, sampling trees every 1000 generations and using the same partitions and evolutionary models as in the Bayesian analysis. An uncorrelated lognormal clock rate and a Yule birth process tree prior were implemented. Stationarity was ensured by excising the first 10 000 sampled trees, and the remaining ones were employed to obtain Bayesian posterior probabilities (BPPs) of clades that were visualised in the highest clade probability tree with mean node heights with TreeAnnotator v1.7.4 (available from the BEAST package).

All Bayesian and BEAST analyses were carried using the University of Oslo Bioportal website (http://www.bioportal.uio.no/). RaxML analyses were performed in the CIPRES cluster website (Miller *et al.*, 2010; http://www.phylo.org/sub_sections/portal/).

Two nodes were calibrated, one separating the Australian species of *Ontsira* from the remaining doryctine taxa, and the other one the most recent common ancestor (MRCA) of the *Aivalykus* + *Ecphylus* clade, using the same ages employed in Ceccarelli & Zaldívar-Riverón's (2013) Bayesian relaxed molecular clock analysis. On the one hand, the most basal node in the tree separating the Australian species of *Ontsira* from the remaining taxa was set to have a mean age of 46 Ma and used a normal distribution and three standard deviations. This calibration was selected based on a previous age estimate for the split between an Australian and a South American doryctine clade (Zaldívar-Riverón *et al.*, 2008), which is congruent with the separation of these two Gondwanan regions (Woodburne & Case, 1996). The MRCA of the *Aivalykus* + *Ecphylus* clade, on the other, was based on two Dominican amber fossil species (Muesebeck, 1960; Zuparko & Poinar, 1997), and was calibrated to have a mean of 17.5 Ma, which used a normal distribution and one standard deviation.

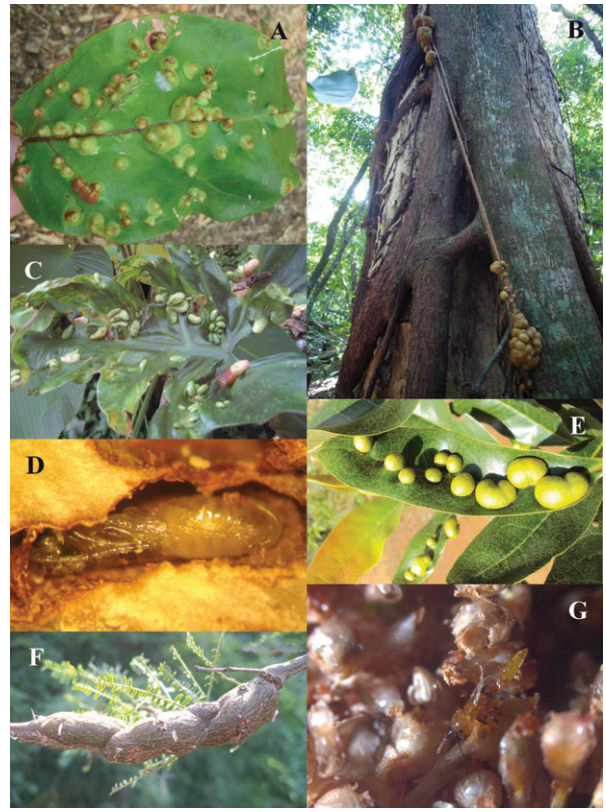

Fig. 1. Photographs showing galls on host plant species from wich doryctine taxa (in parentheses) have been reared. (A) Leaf galls on *Coccoloba barbadensis* Jacquin (*Allorhogas coccolobae* Martínez and Zaldívar-Riverón), Jalisco, Mexico; (B) aerial root galls on *Ficus obtusifolia* Kunth (*Labania* sp.), Costa Rica; (C) leaf galls on *Philodendron radiatum* Schott (*Monitoriella elongata* Hedqvist), Chiapas, Mexico; (D) pupa of *Percnobracon* sp. in a stem gall of *Prosopis caldenia* Burkart; (E) leaf gall on *Duguetia furfuracea* St. Hill. (*Mononeuron duguetiae* Fischer), Sao Carlos, Brazil; (F) stem gall on *Pr. caldenia* (*Percnobracon* sp.), La Pampa, Argentina; (G) brachypterous male of *Psenobolus aff. parapygmaeus* Ramírez and Marsh in syconia of *Ficus crocata* (Miquel) Martius ex Miquel, Mpio. Coyuca de Catalán, Guerrero, Mexico.

Taxonomic descriptions

The specimens examined in this study are deposited in the following collections: Colección Nacional de Insectos, Instituto de Biología, Universidad Nacional Autónoma de México, Mexico (IB-UNAM); Museo Argentino de Ciencias Naturales 'Bernardino Rivadavia', Buenos Aires, Argentina (MACN); Zoological Institute, Russian Academy of Sciences (ZISP); the University of Wyoming Insect Museum, USA (UWIM); and Museum für Naturkunde, Humboldt Universität, Berlin, Germany. The terminology employed in the description of new taxa follows Sharkey & Wharton (1997). Belokobylskij & Tobias's (1998) wing vein terminology is included in parentheses. Digital colour pictures were taken at IB-UNAM with a Leica Z16 APO-A stereoscopic microscope, a Leica DFC295/DFC290 HD camera, and the Leica Application Suite program. Digital

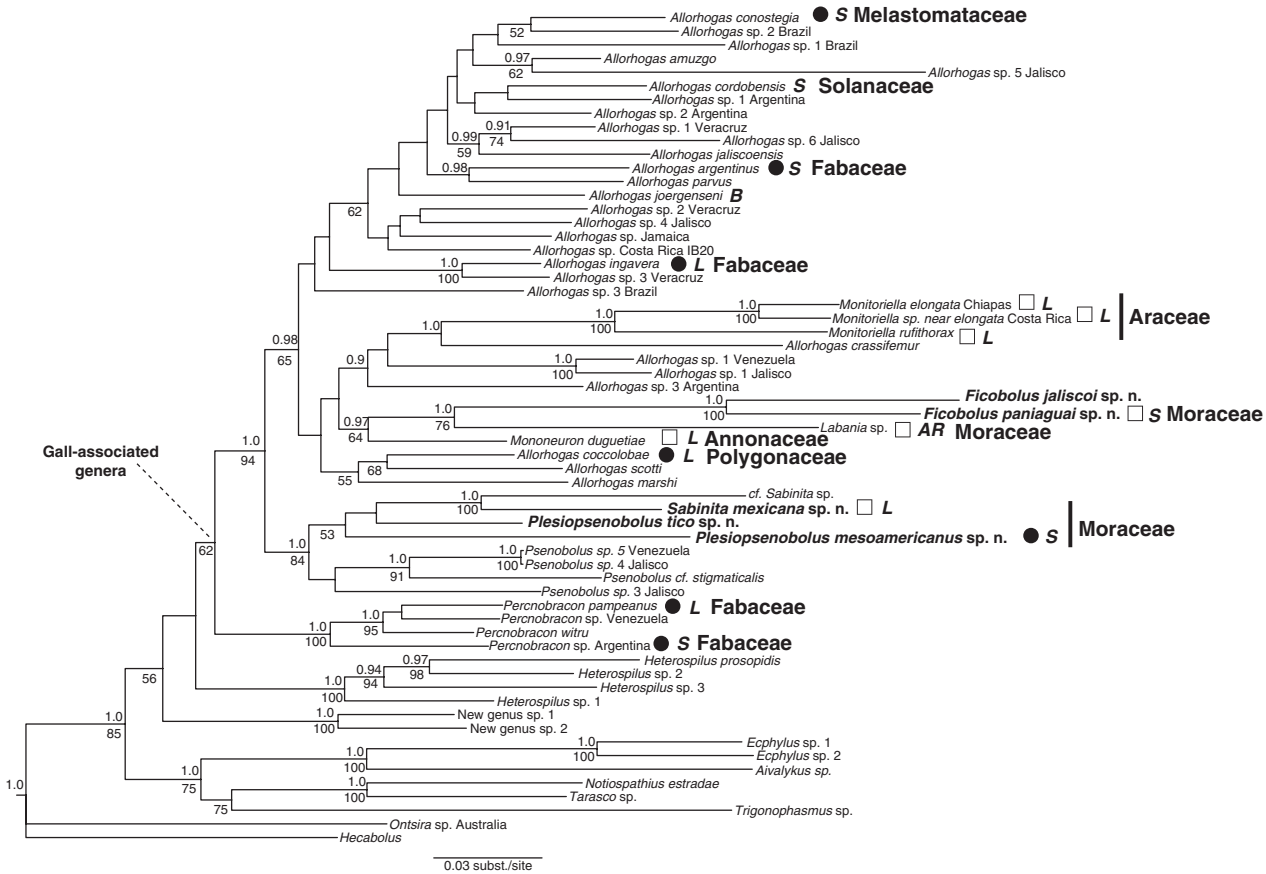

Fig. 2. Bayesian phylogram of Doryctinae derived from the analysis with the *all* dataset. Posterior probability of clades ≥0.9 are shown above branches. Bootstrap values ≥50 obtained from the ML analysis with the *alldata* set are shown below branches. Plant family names are given for terminal taxa with rearing records. AR, aerial root; B, bud; L, leaf; S, stem; black circle, inquiline/parasitoid; hollow square, gall inducer.

photographs were taken with a PHILIPS xl30 scanning electron microscope (SEM). Specimens for SEM images were coated with gold–palladium with a Thermo® VG Scientific SC7620 coater. DNA voucher and GenBank accession numbers for some of the type specimens are included in the descriptions.

Results

Phylogenetic relationships

The concatenated matrix containing all of our gathered data (*all* dataset) consisted of 61 terminal taxa and 2112 nucleotide positions. The Bayesian phylogram derived from the analysis with the *all* dataset is shown in Fig. 2. The Bayesian and ML topologies reconstructed with the remaining datasets are shown in Figure S1. The Bayesian and ML phylograms recovered by the *all* dataset were mostly concordant. Moreover, the phylogenies recovered by the datasets with different levels of missing taxa and characters did not have conflicting significantly/highly supported relationships among them and with respect to the above two topologies.

A clade with the species belonging to the six gall-associated genera, with *Heterospilus* as its sister group, was recovered by nine of the ten analyses performed, although in most cases with nonsignificant/low support. Within the gall-associated clade, a monophyletic *Percnobracon* generally appeared at the base, followed by a clade with eight of the ten species assigned to *Psenobolus*. This *Psenobolus* clade was divided into two subclades whose species are morphologically well differentiated (see below). The remaining gall-associated taxa were grouped in two clades in all analyses. One of these clades had 21 of the 28 species assigned to *Allorhogas*, whereas the other one contained the remaining two species assigned to *Psenobolus*, the included species of *Labania* and *Monitoriella, Mono. duguetiae* and seven species of *Allorhogas*. However, the Bayesian chronogram reconstructed with BEAST placed three of the latter species of *Allorhogas* within the main clade of this genus.

The results of the SS, SH and AU tests of alternative topologies are shown in Table S5. The two tests statistically rejected the topologies constraining the species assigned to *Allorhogas* as monophyletic, as well as the topologies constraining the monophyly of *Allorhogas* + *Mono. duguetiae*. Monophyly of

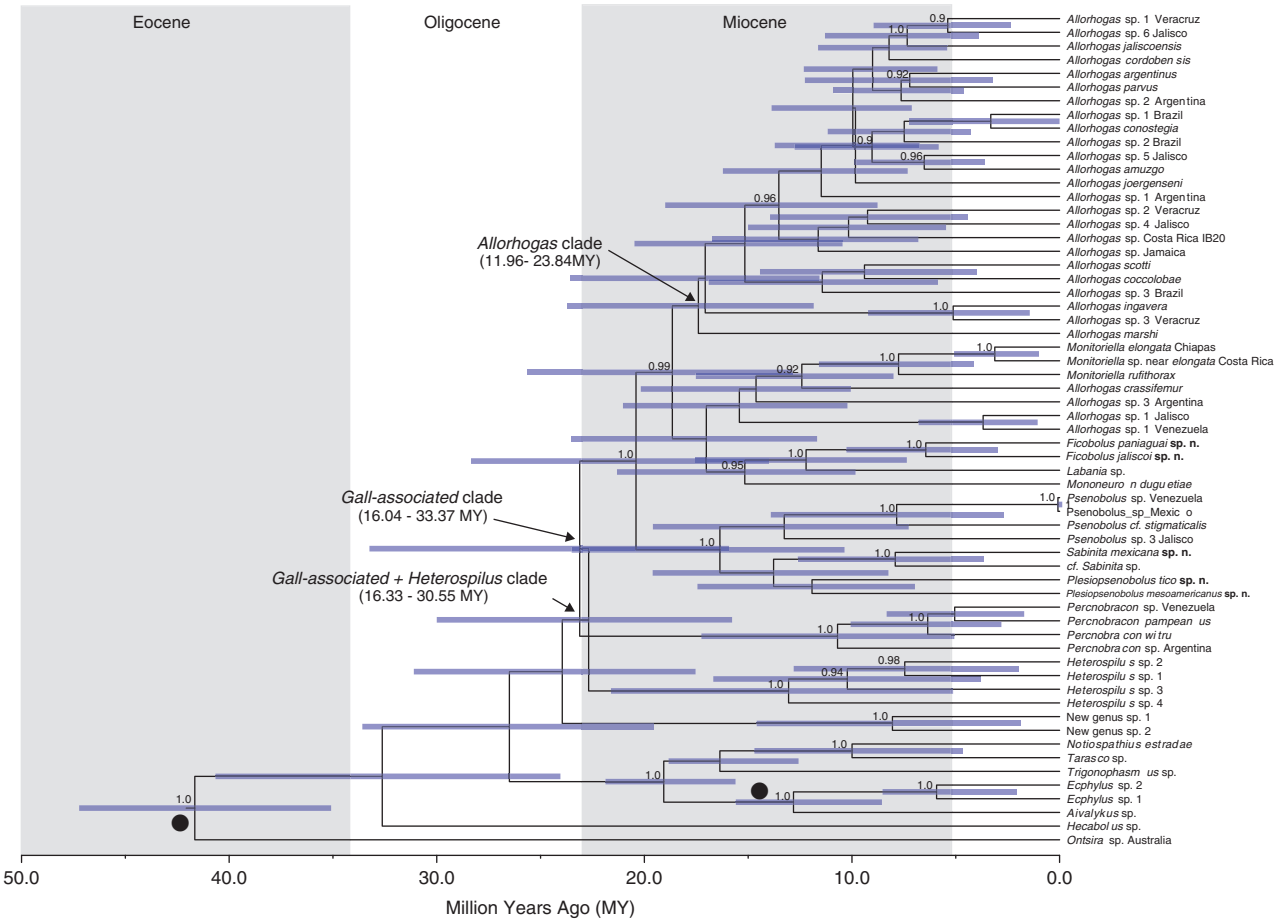

Fig. 3. Chronogram derived from the Bayesian relaxed molecular clock analysis performed with the *all* dataset of Doryctinae, showing divergence time estimates for selected clades. Bayesian posterior probability of clades ≥0.9 are shown. Black circles indicate the two nodes that used fossil calibrations.

our ten specimens assigned to *Psenobolus*, however, was not statistically rejected by the above two tests.

Divergence-time estimates

The ultrametric tree recovered by the Bayesian relaxed molecular clock analysis performed with the *all* dataset is shown in Fig. 3. On the one hand, the most recent common ancestors (MRCA) of the gall-associated clade and of this clade + *Heterospilus* both appear to have diverged during the middle Miocene to late Oligocene, 16.0–33.37 and 16.33–30.55 Ma, respectively. The MRCAs of the main *Psenobolus* and *Allorhogas* clades, on the other, were estimated to have diverged during the middle Miocene to early Oligocene, 10.48–23.63 and 11.96–23.84 Ma, respectively, whereas the MRCA of *Monitoriella* appears to have diverged more recently, during the Pleistocene to middle Miocene 4.27–11.72 Ma. The range estimated for the MRCA of *Percnobracon* was estimated to have diverged during the early to late Miocene 5.19–17.38 Ma.

Discussion

Monophyly of gall-associated Doryctinae

Most of our phylogenetic analyses, which were performed using different combinations of missing taxa and characters, recovered a clade with the species of the six gall-associated doryctine genera included. Compared to our two previous phylogenetic studies (Zaldívar-Riverón *et al.*, 2007, 2008), in this work we employed two additional gene markers and a considerably higher number of representatives of each genus, which covered most of their known morphological diversity. This and the exclusive biology shared by the taxa involved within the subfamily led us to confirm the monophyly of this group.

The external morphology of most of the currently recognised gall-associated doryctine genera differs considerably, and in our examination of all the available specimens we could not find any consistent synapomorphy or combination of characters that distinguish them from the remaining doryctine taxa. The association with galls is therefore proposed here as their only

known synapomorphy, awaiting further studies of additional character systems, such as larval features, genitalia, venom gland apparatus and ovipositor structure, which might allow the discovery of additional diagnostic features. The tribal status of the gall-associated doryctine genera also needs to be assessed based on further phylogenetic studies that include members of all the currently recognised supraspecific taxa within the subfamily.

Generic limits

The main external morphological diagnostic features that distinguish each of the gall-associated doryctine genera recognised in this study are listed in the key to genera (see below). *Percnobracon* consistently appears as monophyletic and at the base of the gall-associated clade, and is one of the most morphologically distinctive genera. Among the main features that characterise it we found a novel, consistent putative synapomorphy: the dorsal side of forewing with large bare areas.

The validity of the monotypic *Mononeuron* with respect to *Allorhogas* is also confirmed based on the relationships recovered. In the redescription of this genus, Nunes *et al.* (2012) found that *Mono. duguetiae* shares various morphological features with *Allorhogas*, although they recovered it as sister to a *Monitoriella* + *Labania* clade. Moreover, despite the fact that our molecular phylogenetic analyses only included one undescribed species of *Labania*, this genus also appears to be morphologically well defined and therefore is probably monophyletic. Surprisingly, all of the topologies placed the specimen of *Labania* in a clade together with the two representative species of a new genus (see below), and with *Mono. duguetiae* at the base of all of them.

Allorhogas is one of the most speciose doryctine genera in the Neotropics perhaps only after *Heterospilus* and *Notiospathius*. This neglected genus is currently receiving more attention, and several new species have been described during the last decade (Martínez *et al.*, 2008; Penteado-Dias & de Carvalho, 2008; Chavarría *et al.*, 2009; Centrella & Shaw, 2010, 2013; Martínez *et al.*, 2011; Martínez & Zaldívar-Riverón, 2013). These and previous studies (e.g. Marsh, 1993) have reported important variation in several key morphological features within the genus, although the monophyly of the group has never been investigated. In our phylogenetic analyses, *Allorhogas* was recovered as nonmonophyletic, and the tests of alternative topologies also rejected its monophyly. However, several of the relationships involved were not significantly supported, with the number of species nested outside the main *Allorhogas* clade varying depending on the amount of missing taxa/characters included in the analyses. This nonmonophyly could be due to the lack of phylogenetic signal in the gene markers employed, although a re-examination of the species placed outside the main *Allorhogas* clade in our analyses showed that one of them, *A. crassifemur* Martínez and Zaldívar-Riverón, has at least two features that are absent in the remaining species of the genus: first flagellomere distinctly longer than the second one and convergent striations on apical area of first metasomal tergite.

Morphological differences between the species of *Allorhogas* and *Donquickeia* are also unclear. Marsh (1993) erected *Quickia* but subsequently changed its name to *Donquickeia* (Marsh, 1997a), based on two species from Brazil. In his description, however, the author did not mention any diagnostic feature that distinguishes this genus from any other doryctine taxon except *Semirhytus* Szépligeti. A further study including species of *Donquickeia*, a considerably larger number of species of *Allorhogas* and additional gene markers is therefore needed to clarify the validity of the former genus, as well as the composition and limits of the second one.

The relationships recovered grouped the species assigned to *Psenobolus* in various morphologically and biologically distinctive clusters. We propose three new genera (see below), each consisting of species that appear to be associated with different organs on *Ficus* species. Based on examination of the lectotype and paralectotype of *Ps. pygmaeus* Reinhard (Fig. 4A–D), the type species of the genus, *Psenobolus* s.s. is delimited to contain its previously recognised species except *Pl. plesiomorphus* van Achterberg and Marsh. Rearing records for *Psenobolus* s.s. are restricted to syconia (van Achterberg & Marsh, 2002). Members of the above genus are sister to a clade with species of two of the newly described genera. One of these, *Plesiopsenobolus* **gen.n.**, comprises two new species and *Pl. plesiomorphus* **comb.n.**, whereas the second, *Sabinita* **gen.n.**, comprises a new species and a species that remains undescribed. The two aforementioned new genera do not appear as monophyletic in our analyses and their proposed species show some distinct morphological features (see taxonomic part). Members of each of these genera, however, share various key diagnostic features and we have therefore decided not to recognise additional genera until further evidence helps us to clarify the status of the taxa involved. The third new genus, *Ficobolus* **gen.n.**, contains the two species that appeared nested in a distantly related clade. One species of *Ficobolus* **gen.n.** and one of *Plesiopsenobolus* **gen.n.** were both reared from the same stem galls, and preliminary observations suggest that the former is a gall former and the second an inquiline (P.E. Hanson, unpublished data), although this requires confirmation. In addition, one species of *Sabinita* **gen.n.** was reared from leaf galls.

Evolution of gall formation

Our results strongly support a sister relationship between members of Heterospilini, represented here by species of the cosmopolitan *Heterospilus*, and the gall-associated doryctines. *Heterospilus* is by far the most speciose member of Heterospilini, which has ten recognised genera (Belokobylskij, 2006; Marsh *et al.*, 2013), and is one of the most species-rich braconid genera in the Neotropics with perhaps hundreds of species remaining to be described for this region. Our analyses and the extraordinary species richness in *Heterospilus* thus indicate that the MRCA of the above two groups could have diverged in the Neotropics during the middle Miocene to late Oligocene, with a rapid origin of the gall-associated doryctine clade occurring during the same period.

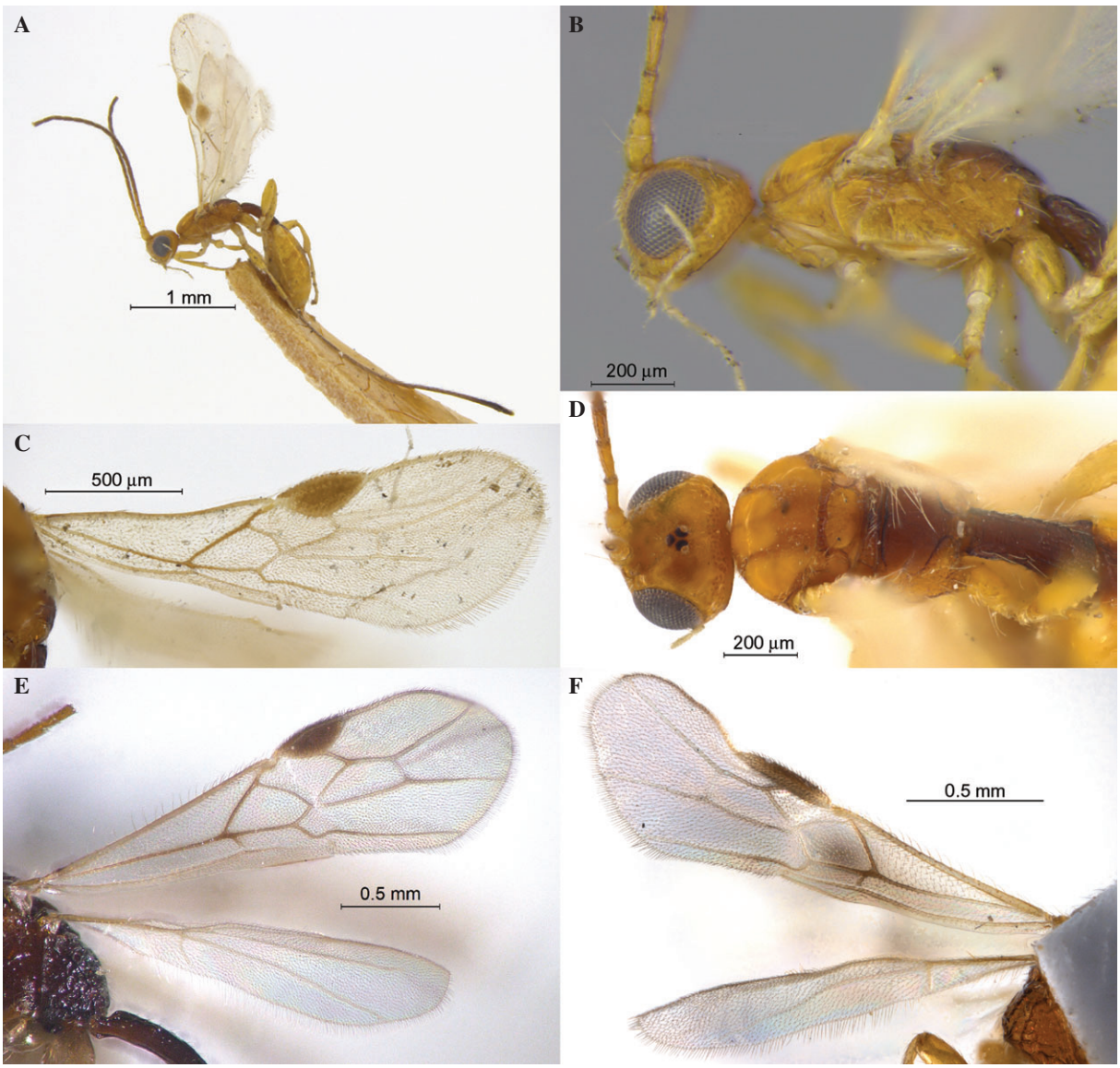

Fig. 4. *Psenobolus pygmaeus* Reinhard. Paralectotype, female: (A) habitus (lateral view); (B) head and mesosoma (lateral view); (C) forewing; (D) head and mesosoma (dorsal view); *Ficobolus paniaguai* **sp.n.** Holotype, female: (E) forewing; *Sabinita mexicana* **sp.n.** Paratype, female: (F) fore and hindwing.

The scarcity of rearing records for most of the species examined here prevented us from thoroughly investigating the evolution of gall association and gall formation within the study group. However, below, we propose some scenarios based on the recovered relationships and the currently gathered biological information. Species with rearing records (host plant family, plant organ where the gall was located and suspected/confirmed biology) included in the Bayesian phylogram derived from the *all* dataset are indicated in Fig. 2.

Percnobracon and *Allorhogas* appear to be the only genera that contain species that are parasitoids (or inquilines) of other gall-forming species, whereas the remaining genera are apparently composed exclusively of gall inducers, although this requires further investigation. Rearing records for *Percnobracon*, which is sister to the remaining genera, indicate that its species do not form the galls from which they are reared, but instead are inquilines or parasitoids of gall-forming dipterans (Cecidomyiidae) (Martínez, 2006). Thus, the basal position of *Percnobracon* is concordant with the hypothesis of an origin of phytophagy in Doryctinae arising from parasitoidism of gall formers (Zaldívar-Riverón *et al.*, 2007).

Allorhogas, however, appears to include both gall inducer and parasitoid/inquiline species. In our analyses the main clade of the genus was deeply nested within the gall-associated doryctine group, with its recorded inquiline/parasitoid species (*A. coccolobae* Martínez and Zaldívar-Riverón, *A. argentinus* Brèthes and *A. ingavera* Marsh) always appearing in separate clades. Further rearing records and analyses with additional

taxon sampling are therefore necessary to investigate whether gall formation was gained and/or lost on various occasions within this genus.

In most gall-associated doryctine genera, host plants appear to be restricted to a single family except in *Allorhogas*, where species are associated with at least eight different plant families (Table S1). However, known gall former species in this genus have been recorded only from three plant families: Fabaceae, Melastomataceae and Rubiaceae. It is possible that adaptation to attacking a wide range of gall-forming species occurring on various plant families could have triggered a higher species diversification in the main *Allorhogas* clade compared to the remaining gall-associated doryctines. Moreover, this could have promoted independent origins of gall formation in at least three different, unrelated plant families.

In contrast, species diversification in the remaining genera that are younger and monophyletic possibly occurred via host shifts within a particular plant taxon and shifts to different plant organs. In particular, despite the scarcity of rearing records, species of *Monitoriella* appear to be gall inducers on leaves, roots, stems and fruits of *Philodendron* and *Anthurium* (Araceae). Moreover, our data reveal an astonishing diversity of associations of closely related but morphologically heterogeneous wasp taxa on different organs of *Ficus*. Further knowledge of the trophic relationships occurring between doryctine and *Ficus* species will undoubtedly help to clarify the evolution of this intricate plant–insect system.

Our preliminary results about the origin and evolution gall formation within the Doryctinae appear to be congruent with those found for the family Cynipidae. In the latter family, the origin of gall formation has been proposed to have arisen from parasitoids of other gall-former insects (Ronquist, 1995; Quicke, 1997), and this biology appears to have been lost in at least three separate lineages (exclusively composed by inquiline species) within the group (Nylander *et al.*, 2004). Moreover, our suggestion about shifts to other plant organs in the gall-associated doryctine taxa is similar to the one proposed for the cynipid genus *Andricus*, where host shifts appear to be less frequent than shifts to other organs on the same host plant (Cook *et al.*, 2002).

Systematic part

Ficobolus Martínez, Belokobylskij et Zaldívar-Riverón, gen.n.

http://zoobank.org/urn:lsid:zoobank.org:act:A91F5FDC-F6C1-424D-90D2-8596D1647D38
(Figs 4E, 5A–F, 6A–F)

Type species. Ficobolus paniaguai Martínez, Belokobylskij et Zaldívar-Riverón **sp.n.**

Diagnosis. Species of this new genus can be distinguished from those of the remaining doryctine genera by having the mesopleuron with an oblique furrow and a distinct frontal cavity laterally margined by a sharp longitudinal carina. They are morphologically similar to species of *Psenobolus* and two genera described below, *Plesiopsenobolus* **gen.n.** and *Sabinita* **gen.n.**, but can be distinguished by having the features mentioned in the key to genera (see below).

Description. Small, body length 1.9–4.1 mm. *Head*: not depressed, transverse. Vertex densely aciculate with fine granulation, occasionally granulate-reticulate or mostly smooth. Ocelli arranged in almost equilateral or isosceles triangle with its base larger than its sides. Frons with distinct and relatively narrow excavation running from lateral ocelli, with distinct, slender and not pronounced median longitudinal keel in its anterior half; with distinct lateral protuberances emarginated by a sharp longitudinal carina. Eyes often with sparse and short setae or almost glabrous. Occipital carina complete, fused with hypostomal carina before mandible. Malar suture absent. Clypeus not high, delineated from face by a distinct furrow, with a fine lower flange. Hypoclypeal depression rather small and rounded. Postgenal bridge wide. Maxillary palpi short, 6-segmented, apical segment as long as fifth segment; labial palpi short, 4-segmented, third segment not shortened. Scape of antenna wide and short, without apical flange and ventroapical lobe, without basal constriction; ventral margin of scape shorter than dorsal one (lateral view). First flagellar segment long, subcylindrical, slightly curved outwards, distinctly longer than second segment. Apical segment pointed apically, without ‘spine’.

Mesosoma: not depressed, short. Neck of prothorax short. Pronotum slightly convex dorsally (lateral view), with a narrow medially and wide laterally anterior curved up flange; pronotal carina absent or present. Pronope absent. Propleural dorsoposterior flange short and wide or narrow. Mesonotum high, almost perpendicularly or roundly elevated above pronotum, mostly granulate or almost smooth. Median lobe of mesonotum with or without distinct median longitudinal furrow, anterolateral corner absent. Notauli complete, deep, wide, not joining and reaching posterior margin of mesoscutum separately or sometimes joining at posterior edge of mesoscutum. Tegula evenly widened distally, not concave along external margin. Scuto-scutellar suture distinct and complete. Prescutellar sulcus (depression) long, with various distinct carinae. Lateral longitudinal flanges on level of prescutellar sulcus low. Scutellar disc slightly convex, not transverse, without lateral carinae. Subalar depression distinct. Mesopleural pit distinct. Mesopleuron irregularly striate and granulate, with oblique depression from mesopleural pit to half the length of sternaulus or incomplete and only present posteriorly. Sternaulus deep, wide and long, running to posterior margin of mesopleuron, distinctly curved up anteriorly, slightly curved posteriorly. Prepectal carina distinct and complete, pronounced ventrally, laterally reaching anterior margin of subalar depression. Postpectal carina absent. Metanotum often with short and rounded median tooth (lateral view). Metapleural flange short and wide, subpointed apically. Propodeum with areas delineated by distinct carinae; lateral tubercles absent; propodeal bridge absent. Propodeal spiracles small and rounded. Metapleuron slightly convex, entirely sculptured.

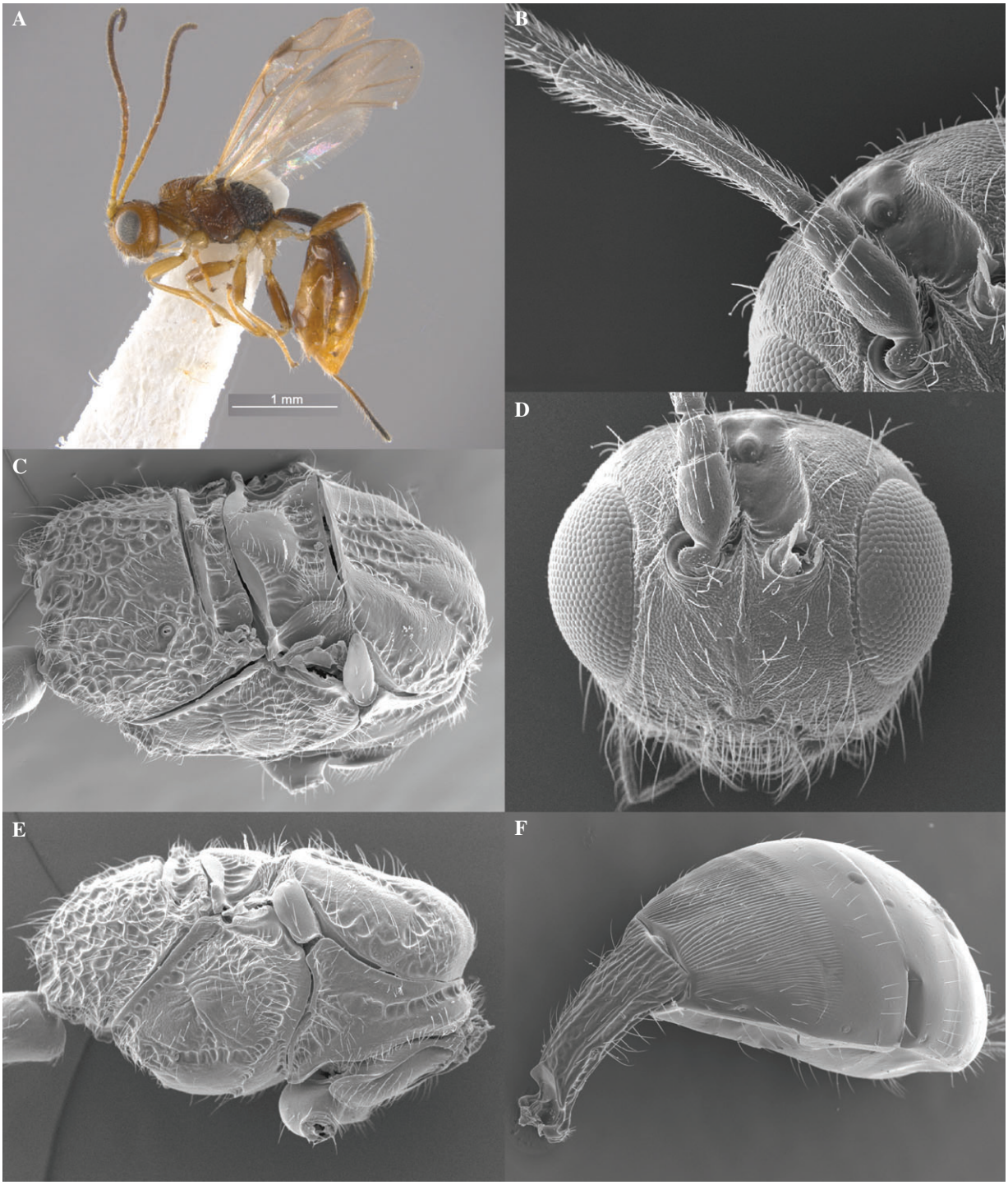

Fig. 5. *Ficobolus paniaguai* **sp.n.** Holotype, female: (A) habitus (lateral view); (B) first and second antennal segment; (C) mesosoma (dorsolateral view); (D) head, frontal view; (E) mesosoma (lateral view); (F) metasoma (dorsolateral view).

Wings: pterostigma of forewing wide and short. Vein r (first radial abscissa) arising from or before middle of pterostigma. Marginal (radial) cell slightly shortened. Veins RS and r-m (both radiomedial) present. Second submarginal (radiomedial) cell long and narrow. Vein m-cu (recurrent) slightly antefurcal. Vein 1cu-a (nervulus) postfurcal. First discal (discoidal) cell petiolate anteriorly. Vein 1RS long. Veins M (basal) and m-cu (recurrent) subparallel or slightly convergent towards

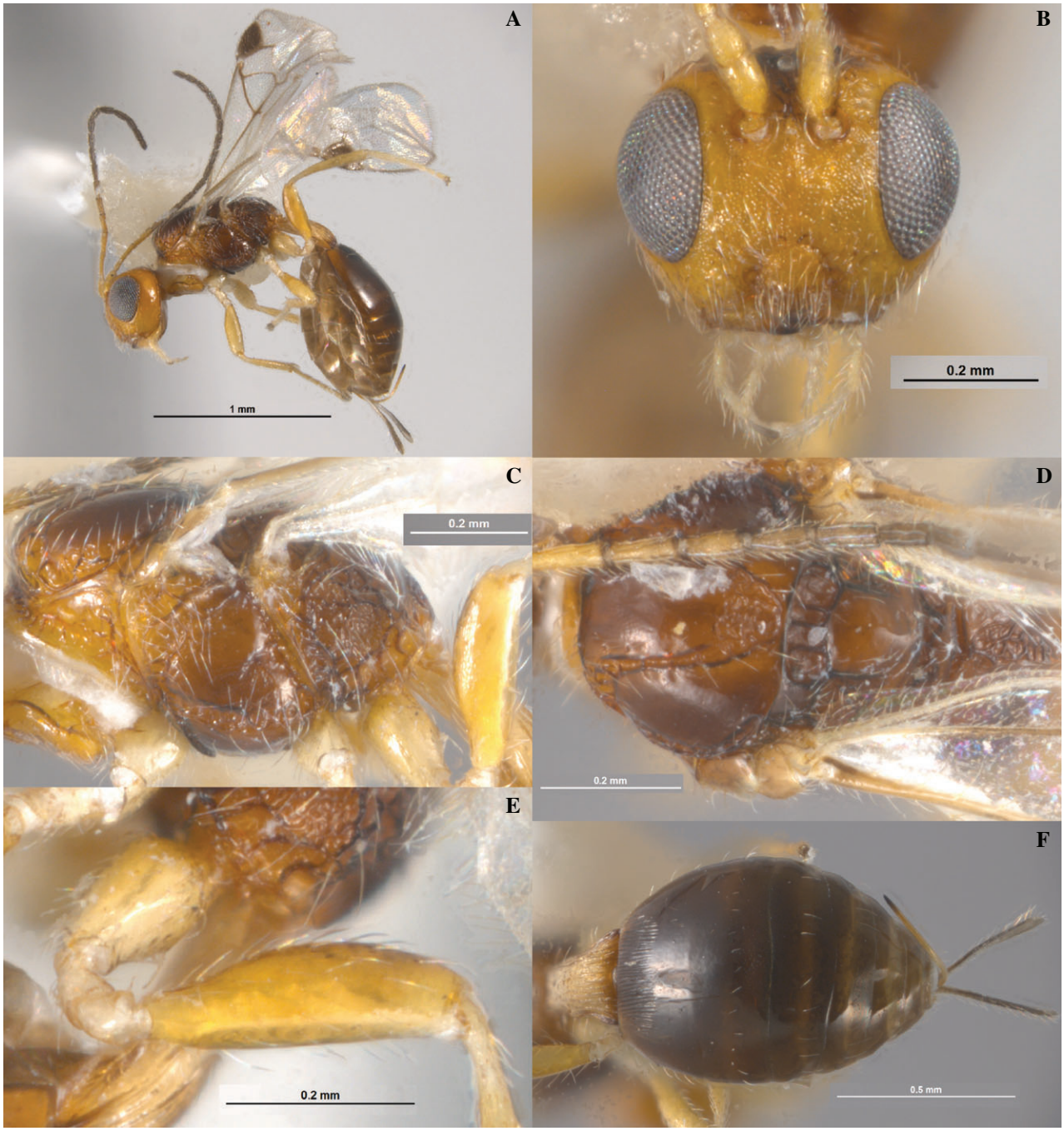

Fig. 6. *Ficobolus jaliscoi* **sp.n.** Holotype, female: (A) habitus (lateral view); (B) head, frontal view; (C) mesosoma (lateral view); (D) mesosoma (dorsal view); (E) hind femur; (F) metasoma (dorsal view).

posterior margin of wing. Vein 2CUb (parallel) not interstitial, distinctly or slightly curved basally. First subdiscal (brachial) cell widely open postero-apically. Vein 2cu-a (brachial) absent. Veins 1a and 2a (transverse anal) absent. Hindwing with three hamuli. Vein C + Sc + R (first abscissa of costal vein) longer than vein SC + R (second abscissa). Vein RS (radial) arising from vein R (costal) far from vein r-m (basal). Marginal (radial) cell slightly widened basally, then more or less distinctly narrowed towards apex, without vein r (additional transverse). Basal (medial) cell not widened from middle towards apex, 7.0–10.0× longer than width, 0.25–0.3× as long as hindwing. Vein cu-a (nervellus) present. Subbasal (submedial) cell long. Vein M + CU (first abscissa of mediocubital vein) not or slightly shorter than vein 1M (second abscissa). Vein m-cu (recurrent vein) long, oblique toward apex of wing, slightly evenly curved or straight. Male hindwing without stigma-like enlargement.

Legs: fore tibia on inner surface with several long and slender spines arranged along its anterior margin in almost vertical line. Fore tarsus ≥1.2× longer than fore tibia. Middle tibia with several spines on anterior surface. Middle tarsal segments short. Hind coxa long and narrow, with distinct basoventral angle but without tubercle. Fore and middle femora with small dorsal protuberances. Hind femur widened and elongate-oval, but in male strongly widened. Hind tibia with area of dense setae on its inner apical quarter. Basitarsus of hind tarsus thickened, 0.5–0.8× as long as second–fifth segments combined. Fifth tarsal segments thickened. Claws short and simple.

Metasoma: first tergite petiolate, long, narrow and distinctly curved. Basal sternal plate (acrosternite) long, 0.6–0.7× as long as first tergite, ending behind spiracles. Dorsope of first tergite small and shallow; basolateral lobes short and wide; spiracular tubercles small, situated in basal 0.4 of tergite; tergites in basal 0.15 with a distinct semi-circular, transverse carina. Second tergite without furrows. Second suture complete, straight and considerably shallow or absent. Third tergite without furrows. Second and third tergites with separate laterotergites, following tergites without separated laterotergites. Third and following tergites with a single transverse line of sparse, long erect setae. Hypopygium widely narrowed towards apex on posterior margin, subpointed medioapically. Ovipositor nodes indistinct. Ovipositor sheaths distinctly shorter than metasoma.

Distribution. Neotropical region (Costa Rica and Mexico).

Biology. The two known species of this genus are associated with species of *Ficus*. The type species, *F. paniaguai* **sp.n.**, was reared from stem galls of *Ficus perforata* Linnaeus (see below).

Etymology. This genus is named after the plant genus from which its type species was reared, *Ficus*, in combination with the last letters of *Psenobolus*, its morphologically similar taxon.

Key to species of *Ficobolus*

1. Transverse diameter of eye 1.6–1.7× longer than temple. Antennae 23–29-segmented. First flagellar segment 1.4–1.6× longer than second one. Vein r (first radial abscissa) arising from middle of pterostigma (Fig. 4E). Hind femur of female 3.5–3.8× longer than wide. First tergite of female 1.6–1.8× longer than apical width. Second suture fine but distinct (Fig. 5F). Vertex densely and finely aciculate, with dense granulation; temple densely and finely granulate-reticulate. Mesoscutum densely and finely granulate, coriaceous laterally, with fine transverse striation anteriorly. Scutellar disc densely and finely coriaceous, sometimes partly smooth. Mesopleuron coarsely striate with dense granulation, only granulate in lower posterior quarter (Fig. 5E). Second tergite entirely and third one on basal 0.25–0.3 densely aciculate. Petiole dark reddish brown (Fig. 5F). Body length 2.7–4.1 mm . . . . . *F. paniaguai* **sp.n.**
– Transverse diameter of eye 1.8–2.0× longer than temple. Antennae 15–17-segmented. First flagellar segment 1.2–1.25× longer than second one. Vein r (first radial abscissa) arising before middle of pterostigma. Hind femur of female 3.1–3.3× longer than wide (Fig. 6E). First tergite of female 1.3–1.5× longer than apical width. Second suture absent (Fig. 6F). Vertex finely coriaceous, usually smooth laterally; temple, mesoscutum and scutellar disc mostly smooth (Fig. 6D). Mesopleuron mostly smooth, partially reticulate and with fine striae (Fig. 6C). Second tergite densely aciculate on basal half, remaining tergites smooth (Fig. 6F). Petiole whitish yellow. Body length 1.9–2.5 mm . . . . . *F. jaliscoi* **sp.n.**

Ficobolus paniaguai Martínez, Belokobylskij et Zaldívar-Riverón sp.n.

http://zoobank.org/urn:lsid:zoobank.org:act:24AA6D9E-1359-4205-85AA-14B12866A4A5
(Figs 4E, 5A–F)

Description. Female. Body length 2.7–3.8 mm; forewing length 2.0–2.6 mm. *Head*: width 1.6–1.8× its median length, 1.1× width of mesoscutum. Head behind eyes (dorsal view) roundly narrowed posteriorly. Transverse diameter of eye 1.6–1.8× longer than temple. Ocellar triangle situated almost on middle of head (dorsal view). Ocelli medium-sized, arranged in triangle with base equal to or slightly larger than its sides. POL 1.2–1.5× Od, 0.2–0.3× OOL. Eye without emargination opposite antennal socket, 1.1–1.2× higher than broad. Malar space 0.4–0.45× height of eye, 0.8–1.0× basal width of mandible. Face without distinct carinae along eyes, with shallow short depressions above clypeus; width of face 1.0–1.1× height of eye, 1.1× height of face and clypeus combined. Diameter of antennal socket about equal to distance between sockets. Clypeus 2.0× wider than its median height. Hypoclypeal depression 0.75–0.85× as wide as distance from edge of depression to eye, 0.4–0.5× width of face.

Antennae slender, filiform, 24–28-segmented, as long as body. Scape 1.6–1.7× longer than maximum width (lateral view), 2.0–2.5× longer than pedicel. First flagellar segment 4.4–4.8× longer than apical width, 1.4–1.6× longer than second segment. Penultimate segment 2.3–2.5× longer than wide, about as long as apical segment.

Mesosoma: 1.7–1.8× its maximum height. Mesoscutum 1.15–1.25× wider than its median length. Median lobe of mesoscutum slightly protruding anteriorly, slightly convex on anterior margin. Notauli distinctly and sparsely crenulate, finely coriaceous between crenulae, not joining, finishing at posterior margin of mesoscutum in a posterior rugose-areolate median area. Prescutellar sulcus (depression) finely granulate-coriaceous or smooth, with four-five coarse carinae, about 0.4× as long as scutellar disc. Metanotum (dorsal view) with distinct and short median carina and two slightly convergent posteriorly lateral carinae, fused with posterior convex area. Sternaulus entirely distinctly and densely crenulate with fine granulation, mostly deep but shallow posteriorly, running along entire length of lower part of mesopleuron.

Wings: forewing 2.8–3.2× longer than maximum width. Pterostigma 2.5–2.8× longer than wide. Vein R1 (metacarp)

1.3–1.5× longer than pterostigma. Vein 3RSa (second radial abscissa) 2.0–2.5× longer than vein r (first abscissa), 0.3–0.4× as long as slightly curved vein 3RSb (third abscissa), 0.7–1.1× as long as vein 2RS (first radiomedial vein). Second submarginal (radiomedial) cell 2.8–3.4× longer than maximum width, 1.3–1.4× longer than first subdiscal (brachial) cell. Vein RS + M (first medial abscissa) slightly sinuate. Vein M + CU (mediocubital vein) almost straight posteriorly. Distance from vein 1cu-a (nervulus) to vein 1M (basal vein) 0.3–0.4× vein 1cu-a (nervulus) length. Hindwing 4.2–4.6× longer than maximum width. Vein M + CU (first abscissa of mediocubital vein) 0.8–0.9× as long as vein M (second abscissa). Vein m-cu (recurrent vein) strongly unsclerotised, slightly postfurcal.

Legs: hind coxa 1.6–1.7× longer than wide (with basoventral angle). Hind femur 3.5–3.8× longer than wide. Hind tarsus 0.85–0.95× as long as hind tibia. Second segment of hind tarsus 0.45–0.50× as long as basitarsus, 1.1–1.2× longer than fifth segment (without pretarsus).

Metasoma: 1.1–1.2× longer than head and mesosoma combined. First tergite distinctly convex (lateral view), slightly widened from base to apex (dorsal view). First tergite 1.6–1.8× longer than its apical width; maximum width 2.3–2.5× minimum width. Median length of second tergite 0.9–1.1× its basal width, 1.2–1.4× length of third tergite. Suture between second and third tergites fine and slightly curved. Ovipositor sheath 0.5–0.6× as long as metasoma, 0.7–1.0× as long as mesosoma, about 0.4× as long as forewing.

Sculpture and pubescence: vertex densely and finely aciculate with dense additional granulation; frons densely granulate laterally, cavity finely coriaceous to smooth, finely granulate laterally. Face densely granulate; temple finely granulate-reticulate. Mesoscutum finely granulate, becoming coriaceous laterally, with fine transverse striation anteriorly on median lobe, coarsely rugose-areolate in wide and short area in medioposterior half of mesoscutum. Scutellar disc finely coriaceous, sometimes mostly smooth. Mesopleuron coarsely striate with dense granulation, only granulate in lower posterior quarter. Propodeum with areas distinctly delineated by carinae; basolateral areas long, entirely rugose-areolate and with granulation; areola long, wide, connected anteriorly with base of propodeum (without basal carina), coarsely rugose-areolate; petiolate area not separated from areola; propodeum in posterior half coarsely rugose-areolate. Hind coxa densely coriaceous dorsally, remaining area granulate-coriaceous. Hind femur densely and distinctly reticulate-coriaceous. First tergite with coarse, sparse and slightly undulate striae, with dense and fine reticulation between striae. Second tergite entirely and third one in basal 0.25–0.3 densely aciculate; apical region of third tergite and remaining tergites smooth. Vertex densely setose, setae directed forwards, glabrous on anterior third. Mesoscutum with long, pale and semi-erect setae along notauli. Hind tibia dorsally with long, dense and semi-erect setae, length of setae 0.5–0.8× maximum width of hind tibia.

Colour: body dark reddish brown or dark brown; head reddish brown, face brownish yellow; mesonotum and often metasoma reddish brown on posterior third; metasoma yellow or brownish yellow in posterior quarter. Antennae yellow in basal 0.4, brown to dark brown in apical 0.6. Palpi yellow. Legs brownish yellow, all tibiae (except pale bases) and apical half of middle femur slightly darker, hind femur mostly dark reddish brown. Ovipositor sheath dark brown. Forewing faintly infuscate. Pterostigma dark brown.

Male. Body length 2.8–4.1 mm; forewing length 2.0–2.8 mm. Head width 1.4–1.6× median length, 1.2–1.3× width of mesoscutum. POL 1.0–1.2× Od. Malar space about half height of eye. Antennae setiform, 23–29-segmented, slightly longer than body. Pterostigma 2.5–2.7× longer than wide. Vein M + CU (first abscissa of mediocubital vein) of hindwing as long as vein M (second abscissa). First tergite 2.0–2.3× longer than apical width. Median length of second tergite 1.2–1.3× its basal width, 1.4–1.5× length of third tergite. Body sometimes light reddish brown, propodeum and first to third metasomal tergites reddish brown to dark reddish brown and partly almost black. Antennae yellow, pale brown in basal half. Otherwise similar to female.

Distribution. Costa Rica.

Biology. A considerable number of specimens belonging to the type series of this species were reared from round stem galls on *Ficus perforata* L. in Alajuela, Costa Rica, during June 2008. A smaller number of specimens of a second species described below, *Pl. mesoamericanus* **sp.n.**, were also reared from the same galls. Observations of the stem galls suggest that *F. paniaguai* is probably the gall inducer and *Pl. mesoamericanus* **sp.n.** might be an inquiline or parasitoid, though this needs to be confirmed.

Etymology. This species is named after Federico Paniagua, who first noticed and collected these remarkable specimens.

Type material. Holotype: female (IB-UNAM). 'Costa Rica, provincia Alajuela, Sarchí Norte, cantón San Juan, Valverde Vega, Distrito Rodriguez, 15.vi.2008, 1050 m a.s.l., F. Paniagua col., ex galls on *Ficus perforata*'.

Paratypes: 17 females, 26 males, same data as holotype (IB-UNAM, MACN, ZISP); two males with DNA voucher nos CNIN25, 1239, GenBank accession nos KJ586721 (*COI*), KC822140 (*wg*), KJ586752 (*16S*), KJ586790 (*28S*).

***Ficobolus jaliscoi* Zaldívar-Riverón et Belokobylskij, sp.n.**
http://zoobank.org/urn:lsid:zoobank.org:act:92C2DC25-FA38-4689-9498-C7B74F41E79B
(Fig. 6A–F)

Description. Female. Body length 2.4–2.5 mm; forewing length 1.3–1.6 mm. *Head*: width 1.7–1.8× median length, 1.2–1.3× width of mesoscutum. Head behind eyes (dorsal view) distinctly roundly narrowed posteriorly. Transverse diameter of eye about 2.0× longer than temple. Ocellar triangle situated almost on middle of head (dorsal view). Ocelli medium-sized, arranged in triangle with base 1.2× its sides. POL 1.5–1.8× Od,

0.3–0.4× OOL. Eye without emargination opposite antennal socket, 1.3× high than broad. Malar space 0.3–0.4× height of eye, 0.8–1.0× basal width of mandible. Face without distinct carinae along eyes, with shallow short depressions above clypeus; face width 0.9× height of eye and 1.1× height of face and clypeus combined. Diameter of antennal socket about equal to distance between sockets. Clypeus 1.5× as wide as its median height. Hypoclypeal depression 0.9–1.0× as wide as distance from edge of depression to eye, 0.4× face width.

Antennae slender, slightly thickened towards apex, 17-segmented, shorter than body. Scape 1.5–1.6× longer than maximum width (lateral view), about 1.5× longer than pedicel. First flagellar segment 5.0–5.5× longer than apical width, 1.2–1.25× longer than second segment. Penultimate segment 2.0–2.5× longer than wide, 0.8–1.0× as long as apical segment.

Mesosoma: length 1.7× its maximum height. Mesoscutum 1.25–1.3× wider than median length. Median lobe of mesoscutum slightly protruding anteriorly, almost straight or slightly convex on anterior margin. Notauli distinctly and sparsely crenulate, finely coriaceous to smooth between crenulae, fused on posterior margin of mesoscutum. Prescutellar sulcus (depression) almost smooth, with three coarse carinae and several fine and incomplete rugulae, 0.45× as long as scutellar disc. Metanotum (dorsal view) with a short median and two subparallel lateral carinae, fused with posterior convex area. Sternaulus distinct and densely crenulate with granulation, mostly deep, but shallow in posterior third, running along entire length of lower part of mesopleuron.

Wings: forewing 2.7–3.0× longer than maximum width. Pterostigma about 2.0× longer than wide. Vein R1 (metacarp) 1.2× longer than pterostigma. Vein 3RSa (second radial abscissa) 2.7–3.8× longer than vein r (first abscissa), 0.4–0.5× as long as slightly curved 3RSb (third abscissa), 1.1–1.2× longer than vein 2RS (first radiomedial vein). Second submarginal (radiomedial) cell 2.5–2.7× longer than maximum width, 1.3–1.4× longer than first subdiscal (brachial) cell. Vein RS + M (first medial abscissa) slightly sinuate. Vein M + CU (mediocubital vein) almost straight posteriorly. Distance from vein 1cu-a (nervulus) to vein 1M (basal vein) about 0.5× vein 1cu-a (nervulus) length. Hindwing 4.2–4.5× longer than maximum width. Vein M + CU (first abscissa of mediocubital vein) about as long as vein M (second abscissa) (until basal vein). Vein m-cu (recurrent vein) strongly desclerotised, slightly postfurcal, straight.

Legs: hind coxa 1.4–1.5× longer than wide (with basoventral angle). Hind femur 3.1–3.3× longer than wide. Hind tarsus 1.0–1.1× longer than hind tibia. Second segment of hind tarsus 0.6–0.7× as long as basitarsus, 1.1–1.3× longer than fifth segment (without pretarsus).

Metasoma: about 1.1× longer than head and mesosoma combined. First tergite slightly convex (lateral view), distinctly and almost linearly widened from base to apex (dorsal view). First tergite 1.3–1.5× longer than its apical width; maximum width of tergite 2.3–2.5× its minimum width. Median length of second tergite 0.8–0.9× its basal width, 1.3–1.5× length of third tergite. Second suture indistinct. Ovipositor sheath 0.35–0.4× as long as metasoma, 0.6–0.7× as long as mesosoma, about 0.3× as long as forewing.

Sculpture and pubescence: vertex finely coriaceous, usually smooth laterally; frons densely and finely granulate laterally, its cavity finely granulate-coriaceous. Face granulate; temple mostly smooth. Mesoscutum mostly smooth, finely granulate-coriaceous near notauli posteriorly, coarsely rugose-areolate in wide area in medioposterior 0.3 of mesoscutum. Scutellar disc entirely smooth. Mesopleuron mostly smooth, partly reticulate and with fine striae. Propodeum with areas distinctly delineated by carinae; basolateral areas short and semi-rounded, rugulose-reticulate, smooth anteriorly; areola long and wide, connected with base of propodeum anteriorly (witout basal carina), coarsely rugose-areolate; petiolate area not separated from areola; propodeum in posterior half coarsely rugose-areolate. Hind coxa finely coriaceous dorsally, remaining area coriaceous to smooth. Hind femur finely coriaceous dorsally, smooth ventrally. First tergite with coarse, rather sparse and almost straight striae, distinctly reticulated between striae. Second tergite in basal half densely aciculate, remaining area smooth. Remaining tergites smooth. Vertex densely and entirely setose, setae directed forwards. Mesoscutum with short, pale and semi-erect setae along notauli and edges. Hind tibia dorsally with long, relatively dense and semi-erect setae, length of setae 0.4–0.6× maximum width of hind tibia.

Colour: head and prothorax yellow to brownish yellow or brownish orange. Mesosoma mostly reddish brown, faintly infuscate posteriorly or ventrally. Petiole whitish yellow, remaining tergites of metasoma dark brown, turning paler posteriorly. Antennae mostly brown to dark brown, fourth-sixth basal segment yellow to yellowish brown. Palpi pale yellow. Legs yellow to brownish yellow, hind femur and tibia slightly darker, basal parts of tibiae and all tarsi paler. Ovipositor sheath pale brown in basal half, dark brown in apical half. Forewing sub-hyaline. Pterostigma entirely dark brown.

Male. Body length 1.9 mm; forewing length 1.3 mm. Transverse diameter of eye about 1.8× longer than temple. Antennae not thickened towards apex, 15-segmented. First flagellar segment about 6.5× longer than apical width. Penultimate segment 3.2× longer than wide. Propodeum with very short basal carina separating irregular areola from anterior margin of propodeum. Mesoscutum and scutellar disc mostly smooth. Vein R1 (metacarp) 1.3× longer than pterostigma. Second submarginal (radiomedial) cell about 3.0× longer than maximum width. Hind femur distinctly thickened, 2.3× longer than wide. First metasomal tergite less evenly widened, with distinct spiracular tubercles, about 1.6× longer than apical width. Otherwise similar to female.

Distribution. Mexico.

Biology. The three type specimens of *F. jaliscoi* were collected at the beginning of the rainy season in 2009 using yellow pan traps, which were placed near an unidentified species of *Ficus*.

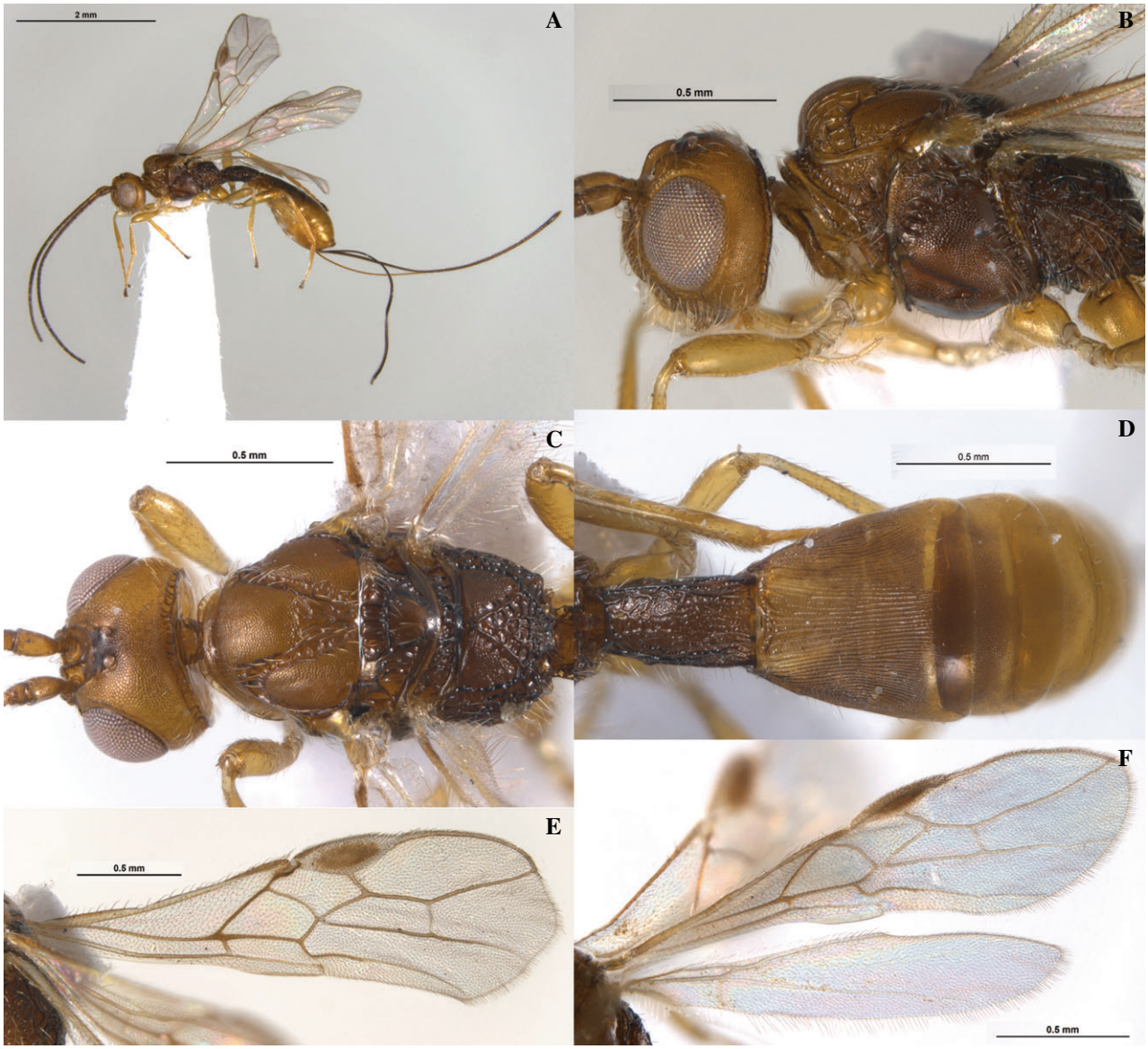

Fig. 7. *Plesiopsenobolus mesoamericanus* **sp.n.** Paratype, female: (A) habitus (lateral view); (B) mesosoma (lateral view); (C) mesosoma (dorsal view); (D) metasoma (dorsal view); (E) forewing; *Plesiopsenobolus tico* **sp.n.** Paratype, female: (F) fore- and hindwings.

Etymology. This species was named after the state of Jalisco, the Mexican state where the type material of this species was collected.

Type material. Holotype: female (IB-UNAM). 'México, Jalisco. Est. Chamela. Camino a Chachalaca, 19.49934–105.03833, 56 m a.s.l., 24–25.vi.2009. Platos amarillos, Selva baja-med., Cham 007A, Clebsch/Zaldívar/Polaszek'; DNA voucher no. ASDOR447, GenBank accession nos HQ200990 (*COI*), HQ200629 (*28S*).

Paratypes: one female, one male (IB-UNAM), same data as holotype; DNA voucher nos ASDOR446, 448, GenBank accession nos HM434540, HQ200991 (*COI*).

***Plesiopsenobolus* Belokobylskij, Martínez et Zaldívar-Riverón, gen.n.**

http://zoobank.org/urn:lsid:zoobank.org:act:B3EFADC5-ABC7-4F56-B72B-1DAA56C2C7E7

(Figs 7A–F, 8A–D)

Type-species. Plesiopsenobolus mesoamericanus **sp.n.**

Diagnosis. This genus is morphologically similar to *Psenobolus*, *Ficobolus* and *Sabinita* **gen.n.**, although they can be distinguished by having the features mentioned in the key to genera (see below).

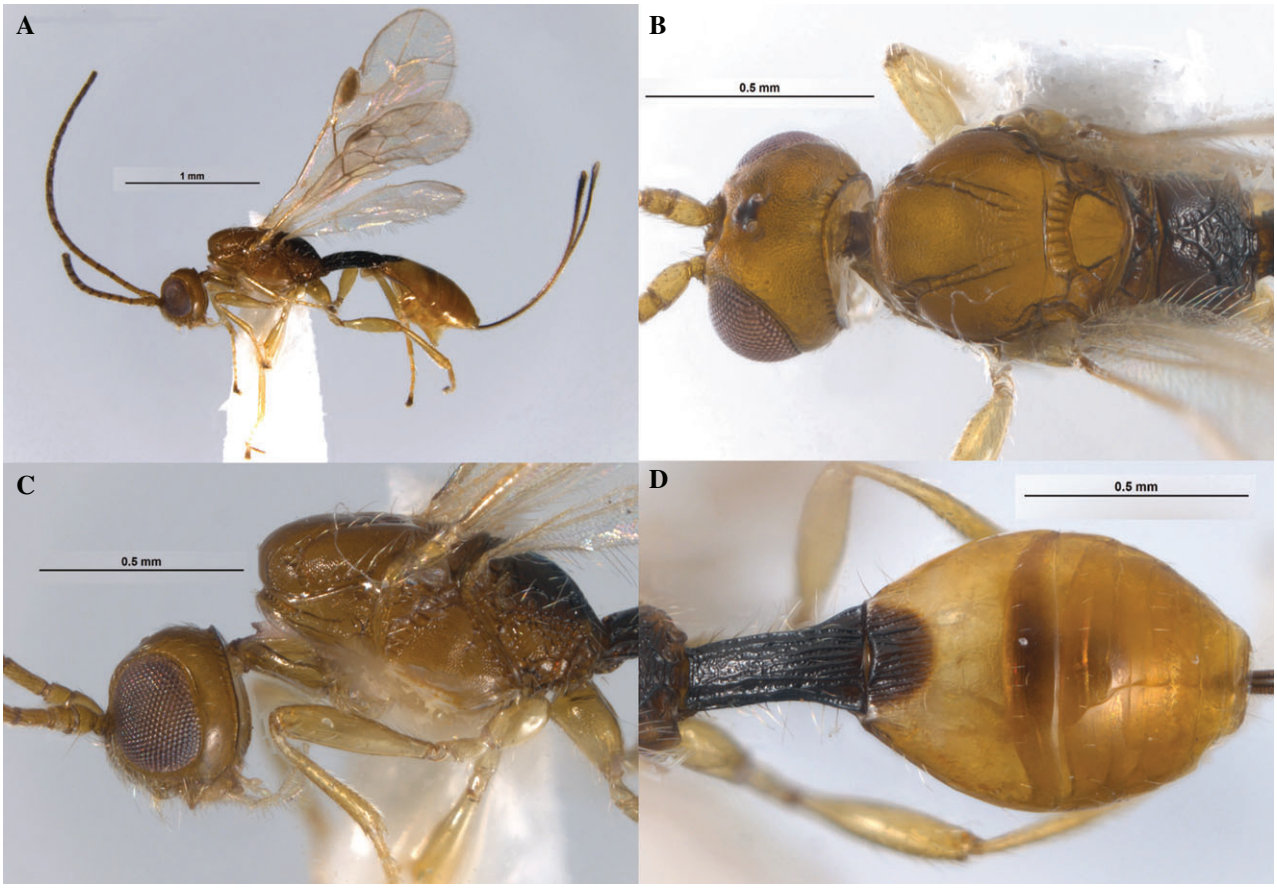

Fig. 8. *Plesiopsenobolus tico* **sp.n.** Paratype, female: (A) habitus (lateral view); (B) mesosoma (lateral view); (C) mesosoma (dorsal view); (D) metasoma (dorsal view).

Description. Small, length 1.9–3.8 mm. *Head*: not depressed, transverse. Vertex densely granulated or coriaceous. Ocelli arranged in triangle with base 1.2–1.3× its sides, or sometimes in almost equilateral triangle. Frons with distinct and wide excavation running from lateral ocelli, with a narrow, long longitudinal keel, with distinct lateral protuberances often emarginated dorsally by incomplete longitudinal carina. Eyes mostly glabrous. Occipital carina coarse, dorsally complete, fusing with hypostomal carina before mandibles. Malar suture absent. Clypeus high, delineated from face laterally and dorsally by distinct or fine furrows, respectively, without or with a fine lower flange. Hypoclypeal depression small and rounded. Postgenal bridge wide. Maxillary palpi short, 6-segmented, sixth (apical) segment about as long as fifth segment; labial palpi short, 4-segmented, third segment not shortened. Scape of antenna wide and long, with fine apical flange but without ventroapical lobe and basal constriction; ventral margin of scape 0.7–0.85× as long as dorsal margin (lateral view). First flagellar segment subcylindrical, not curved, equal to or slightly longer than second segment. Apical segment pointed apically, without 'spine'.

Mesosoma: not depressed, elongate. Neck of prothorax short. Pronotum strongly or distinctly convex dorsally (lateral view), with short and distinct curved up anterior flange; submedian pronotal carina distinct. Pronope absent. Propleural dorsoposterior flange long or short and wide. Mesonotum highly and almost perpendicularly elevated above pronotum, mainly granulate or granulate-coriaceous. Median lobe of mesonotum without median longitudinal furrow, anterolateral corner wide and obtuse. Notauli complete, deep and wide. Tegula distinctly widened distally, not concave along outer margin. Scuto-scutellar suture distinct and complete. Prescutellar sulcus (depression) long, with several carinae. Lateral longitudinal flanges on level of prescutellar sulcus very low. Scutellar disc slightly convex, slightly shorter than or as long as wide, without distinct lateral carinae. Subalar depression distinct and wide or narrow. Mesopleural pit fine. Mesopleuron without any depression. Sternaulus shallow, wide or narrow, short, slightly curved or straight, oblique. Prepectal carina distinct and complete, reaching lower margin of subalar depression or upper margin or sternaulus. Postpectal carina absent. Metanotum without median tooth (lateral view). Metapleural flange long, narrow in lateral and posterior views, subpointed apically. Propodeum with areas delineated by distinct carinae, areola large; lateral tubercles usually absent or sometimes low and obtuse; propodeal bridge absent. Propodeal

spiracles small and rounded. Metapleuron slightly convex, entirely sculptured.

Wings: Pterostigma of forewing narrow and long, or wide and short. Vein r (first radial abscissa) arising slightly before or from middle of pterostigma. Marginal (radial) cell not shortened. Veins 2RS and r-m (first and second radiomedial veins) present. Second submarginal (radiomedial) cell wide, long or short. Vein 1m-cu (recurrent vein) interstitial or antefurcal. Vein 1cu-a (nervulus) postfurcal. First discal (discoidal) cell petiolate anteriorly, vein 1RS (petiole of discoidal cell) long. Veins 1M (basal) and 1m-cu (recurrent) slightly divergent posteriorly or subparallel. Vein 3CU (parallel vein) not interstitial, distinctly curved basally. First subdiscal (brachial) cell open postero-apically, vein 2cu-a (brachial vein) completely absent. Vein 1a and 2a (transverse anal veins) absent. Hindwing with three hamuli. Vein C + Sc + R (first abscissa of costal vein) 1.0–1.4× longer than vein SC + R (second abscissa). Vein RS (radial vein) arising from vein R (costal vein) far from vein r-m (basal vein). Marginal (radial) cell slightly widened basally, distinctly narrowed towards apex, without vein r (transverse vein). Basal (medial) cell not widened from middle towards apex, 10.0–15.0× longer than wide, about 0.3× as long as hindwing. Vein cu-a (nervellus) present. Subbasal (submedial) cell long. Vein M + CU (first abscissa of mediocubital vein) 0.5–0.7× as long as vein M (second abscissa). Vein m-cu (recurrent vein) long, subvertical, slightly curved towards wing apex. Hindwing of male without stigma-like enlargement.

Legs: fore tibia on inner surface with several long and slender spines arranged in a vertical line. Fore tarsus 1.1–1.5× longer than fore tibia. Middle tibia with several spines on anterior surface. Middle tarsal segments long. Hind coxa long and wide, with a distinctly rounded baso-ventral angle but without tubercle. Fore and middle femora without dorsal protuberances. Hind femur narrow and elongated. Hind tibia without comb of dense and long setae along its inner distal margin. Basitarsus of hind tarsus 0.5–0.55× as long as second-fifth segments combined. Fifth tarsal segments slightly thickened. Claws large and simple.

Metasoma: first tergite petiolate, long or medium size, wide or narrow, slightly convex dorsally. Basal sternal plate (acrosternite) distinctly elongated, 0.7–0.75× as long as first tergite, prolonged distinctly behind spiracular level. Dorsope of first tergite very small, almost indistinct; basolateral lobes absent; spiracular tubercles almost indistinct, situated on basal 0.3 of tergite; tergite with a fine semi-circular transverse carina basomedially, carina coarse laterally, with fine and almost complete dorsal carinae. Second tergite without furrows. Second suture fine or indistinct, if present, then complete and slightly sinuate. Third tergite without transverse furrows. Second and third or second to sixth tergites with separate laterotergites. Third and remaining tergites with a transverse line of sparse semi-erect setae. Hypopygium on posterior margin not narrowed and truncate apically. Ovipositor with two almost indistinct subapical nodes. Ovipositor sheaths longer than metasoma.

Biology. The species of this genus whose host plant has been recorded are both from *Ficus*: *Pl. mesoamericanus* **sp.** is associated with stem galls and *Pl. tico* with syconia.

Distribution. Neotropical region (Costa Rica and Brazil).

Etymology. This genus is named after the Greek word '*plesios*' (near, close) and the generic name of its related genus, *Psenobolus*.

Comments. Three species are recognised within this genus according to its diagnostic external morphological features, the two species described below from Costa Rica and *Pl. plesiomorphus* (**comb.n.**), from Brazil.

The type species of this genus, *Pl. mesoamericanus* **sp.n.**, differs morphologically in some characters with respect to the remaining two species, *Pl. tico* **sp.n.** and *Pl. plesiomorphus* (see key to species). Further discovery of additional species belonging to this genus will help to clarify whether the latter two species should be placed within *Plesiopsenobolus* or should be regarded as a separate genus.

Key to species of *Plesiopsenobolus*

1. Antennal sockets inserted above middle level of head (lateral view) (Fig. 7B). Head behind eyes slightly narrowed (dorsal view) (Fig. 7C). Notauli wide and coarsely crenulated (Fig. 7C). First metasomal tergite not widened in apical third, short and wide (Fig. 7D); maximum width of first metasomal tergite 1.4–1.6× minimum width (Fig. 7D). Second metasomal tergite entirely and third one distinctly aciculate at least on basal half (Fig. 7D). Body length 3.2–3.8 mm (Fig. 7A) . . . . . *P. mesoamericanus* **sp. n.**

– Antennal sockets inserted on middle level of head (lateral view) (Fig. 8C). Head behind eyes distinctly narrowed (dorsal view) (Fig. 8B). Notauli narrow and finely crenulated (Fig. 8B). First metasomal tergite distinctly widened in apical third, long and narrow (Fig. 8D); maximum width of first metasomal tergite about 2.0× minimum width (Fig. 8D). Only second metasomal tergite aciculate or striate on basal half, third tergite entirely smooth (Fig. 8D). Body length 1.7–2.9 mm (Fig. 8A) 2

2. Ovipositor about 0.9× as long as forewing and distinctly longer than metasoma (Fig. 8A). First flagellar segment as long as second segment 2.5–3.0× longer than its apical width. Transverse diameter of eye (dorsal view) 2.0–2.2× longer than temple (Fig. 8B). Notauli densely crenulated (Fig. 8B). First metasomal tergite longer, 1.7–2.1× longer than apical width (Fig. 8B). Second tergite striate on basal half (Fig. 8B). Body length 2.6–2.9 mm . . . . . *P. tico* **sp. n.**

– Ovipositor about 0.6× as long as forewing and as long as metasoma. First flagellar segment 0.9× as long as second segment, about 3.5× longer than its apical width. Transverse diameter of eye (dorsal view) 2.8× length of temple. Notauli mostly smooth. First metasomal tergite shorter, 1.6× longer than

its apical width. Second tergite striate only basally. Body length 1.9 mm . . . . . *P. plesiomorphus* (van Achterberg and Marsh) **comb.n.**

Plesiopsenobolus mesoamericanus **Belokobylskij, Zaldívar-Riverón et Martínez sp.n.**
http://zoobank.org/urn:lsid:zoobank.org:act:D7CA4798-444D-42AB-83C7-653E2A0C8A7F
(Fig. 7A–E)

Description. Female. Body length 3.2–3.8 mm; forewing length 2.4–3.0 mm. *Head*: width 1.6–1.8× median length, 1.15–1.2× width of mesoscutum. Head behind eyes (dorsal view) slightly and roundly narrowed posteriorly. Transverse diameter of eye 1.9–2.0× longer than temple. Ocellar triangle situated almost on middle of head (dorsal view). Ocelli medium-sized, arranged in triangle with base 1.2–1.3× its sides. POL 1.0–1.5× Od, 0.3–0.5× OOL. Eye without emargination opposite antennal socket, 1.3× higher than broad. Malar space 0.35–0.4× height of eye, 0.8–1.0× basal width of mandible. Face distinctly convex medially (lateral view), without carinae along eyes, with shallow, narrow and short depressions above clypeus; width of face 0.8–0.9× height of eye and almost equal to height of face and clypeus combined. Diameter of antennal socket about equal to distance between sockets. Clypeus 1.3–1.5× wider than its median height. Hypoclypeal depression 0.8–0.9× as wide as distance from edge of depression to eye, about 0.4× width of face.

Antennae slender, filiform, 29–30-segmented, about as long as body. Scape 1.6–1.7× longer than its maximum width (lateral view), 2.0× longer than pedicel. First flagellar segment 3.0–3.5× longer than its apical width, 1.0–1.1× as long as second segment. Penultimate segment 3.0–3.3× longer than width, 0.9–1.0× as long as apical segment.

Mesosoma: short and high, its length 1.6–1.7× maximum height. Mesoscutum 1.25–1.3× wider than its median length. Median lobe of mesoscutum slightly protruding anteriorly, slightly convex on anterior margin. Notauli distinctly and sparsely crenulate, finely coriaceous between crenulae. Prescutellar sulcus (depression) mainly smooth or finely coriaceous, with four coarse carinae, 0.45–0.5× as long as scutellar disc. Metanotum (dorsal view) with a distinct median and two posteriorly convergent lateral carinae, posterior convex area narrow. Sternaulus finely and densely reticulate-granulate, partly or entirely with fine crenulation, running along anterior 0.6–0.7 of lower part of mesopleuron.

Wings: forewing 3.0–3.2× longer than maximum width. Vein R1 (metacarp) 1.3–1.5× longer than pterostigma. Vein 3RSa (second radial abscissa) 2.8–3.4× longer than vein r (first abscissa), 0.5–0.55× as long as straight vein 3RSb (third abscissa), 1.2–1.5× longer than vein 2RS (first radiomedial vein). Second radiomedial vein (r-m) distinctly inclivous. Second submarginal (radiomedial) cell 3.0-3.2× longer than its maximum width, 1.4–1.5× longer than first subdiscal (brachial) cell. Vein RS + M (first medial abscissa) slightly sinuate. Vein M + CU (mediocubital) slightly curved posteriorly. Distance from vein 1cu-a (nervulus) to vein 1M (basal vein) 0.2–0.4× vein 1cu-a (nervulus) length. Hindwing about 5.5× longer than maximum width. Vein M + CU (first abscissa of mediocubital vein) about 0.7× as long as vein 1M (second abscissa) (until basal vein). Vein m-cu (recurrent vein) strongly desclerotised, postfurcal.

Legs: hind coxa 1.4–1.6× longer than wide (with basal angle). Hind femur 3.6–4.0× longer than wide. Hind tarsus 0.9× as long as hind tibia. Second segment of hind tarsus 0.5–0.6× as long as basitarsus, 1.3× longer than fifth segment (without pretarsus).

Metasoma: 1.2–1.4× longer than head and mesosoma combined. First tergite slightly convex (lateral view), slightly and curvedly widened from base to apical third, slightly narrowed towards subapex (dorsal view), 1.8–1.9× longer than apical width, 1.7–1.8× longer than propodeum; maximum width of tergite 1.4–1.6× minimum width. Median length of second tergite almost equal to its basal width, 0.9–1.0× length of third tergite. Ovipositor sheaths as long as or slightly longer than body, 1.7–2.0× as long as metasoma, 1.3–1.4× longer than forewing.

Sculpture and pubescence: vertex distinctly and densely granulate; frons densely granulate laterally, inside cavity finely granulate-coriaceous with fine rugosity medio-anteriorly. Face densely granulate; temple densely and finely granulate-coriaceous. Mesoscutum densely granulate, without striation, rugose-areolate in narrow and short area in medioposterior 0.3 of mesoscutum. Scutellar disc finely coriaceous, partly smooth. Mesopleuron densely reticulate-coriaceous, granulate dorsally, sculpture becoming finer below. Propodeum with areas distinctly delineated by carinae; basolateral areas medium sized, entirely granulate, with short rugosity along carinae; areola long and wide, connected anteriorly with base of propodeum (without basal carina), entirely rugose-reticulate; petiolate area short and transverse; posterior half of propodeum mostly smooth between sparse and distinct carinae. Hind coxae densely and finely granulate. Hind femur entirely reticulate-coriaceous. First metasomal tergite with coarse, sparse and irregular longitudinal striae, and distinct sparse rugosity between striae. Second tergite entirely and third one densely subaciculate in basal 0.5–0.7 densely subaciculate, with fine reticulation between aciculae. Remaining tergites smooth. Vertex densely setose, setae short and directed forwards. Mesoscutum with short, pale and semi-erect setae situated in narrow lines along notauli and along edges. Hind tibia with short, dense and semi-erect setae dorsally, length of setae 0.4–0.5× maximum width of hind tibia.

Colour: head brownish yellow, slightly infuscate dorsally. Metasoma brownish yellow, brown or almost black. Metasoma dark reddish brown or reddish brown with yellow spots, its apical third brownish yellow to yellow. Antennae brown to dark brown, scape and sometimes three basal segments brownish yellow. Palpi yellow. Legs yellow to brownish yellow, tarsal segments dark brown to black. Ovipositor sheaths dark brown to black, brown basally. Forewing subhyaline. Pterostigma brown, paler apically.

Male. Body length 3.2–3.5 mm; forewing length 2.3–2.7 mm. Malar space 0.35–0.4× height of eye. Antennae 27–29-segmented. First flagellar segment 3.3–3.5× longer

than apical width, as long as second segment. Penultimate segment 3.3–3.5× longer than width. Mesosoma length 1.65–1.7× its maximum height. Prescutellar sulcus (depression) with three coarse carinae. Sternaulus running along anterior 0.7 of lower part of mesopleuron. Pterostigma pale brown. Vein R1 (metacarp) 1.4–1.6× longer than pterostigma. Vein 3RSa (second radial abscissa) 3.1–4.2× longer than vein r (first abscissa), 1.4–1.7× as long as vein 2RS (first radiomedial vein). Second submarginal (radiomedial) cell 2.9–3.4× longer than maximum width. Hindwing 4.4–4.7× longer than maximum width. Hind femur slightly thickened, 3.0–3.5× longer than wide. Metasoma 1.2–1.4× longer than head and mesosoma combined. First tergite 1.9–2.0× as long as apical width, 1.5–1.8× longer than propodeum. Third metasomal tergite densely subaciculate in basal 0.7. Otherwise similar to female.

Distribution. Costa Rica.

Etymology. The name of this species refers to Mesoamerica, the region where Costa Rica is located.

Biology. This species and *F. paniaguai* were reared from the same stem galls on *F. perforata* (see above).

Type material. Holotype: female (IB-UNAM). 'Costa Rica, provincia Alajuela, Sarchí Norte, cantón San Juan, Valverde Vega, Distrito Rodriguez, 15.vi.2008, 1050 msnm, F. Paniagua col., ex galls on *Ficus perforata*'.

Paratypes: 20 females, eight males (IB-UNAM, MACN, ZISP). Eight males, 18 females, same data as holotype; one female, 'Costa Rica, Alajuela, V.V. Rodriguez, 6/X/08, 1050 msnm, F. Paniagua', DNA voucher no. CNIN 23, GenBank accession no KJ586720 (*COI*), KJ586789 (*28S*), KJ586751 (*16S*); one female, 'Costa Rica, Alajuela, Valverde Vega, Rodriguez, 1050 msnm, iii.2008, ex. Galls on *Ficus perforata*. F. Paniagua, CNIN 1240'.

Plesiopsenobolus tico Belokobylskij, Zaldívar-Riverón et Martínez sp.n.

http://zoobank.org/urn:lsid:zoobank.org:act:A9A765E1-AF4B-4814-8DE0-BF27D62F9E3E
(Figs 7F, 8A–D)

Description. Female. Body length 2.7–2.9 mm; forewing length 2.1–2.2 mm. *Head*: width 1.7–1.8× median length, 1.1–1.15× width of mesoscutum. Head behind eyes (dorsal view) roundly narrowed posteriorly. Transverse diameter of eye 2.2× longer than temple. Ocellar triangle situated almost on middle of head (dorsal view). Ocelli medium-sized, arranged in almost equilateral triangle. POL about equal to Od, 0.3× OOL. Eye with slight emargination opposite antennal socket, 1.2–1.25× higher than broad. Malar space 0.15–0.2× height of eye, 0.2–0.3× basal width of mandible. Face slightly convex medially (lateral view), without carinae along eyes, with fine depressions above clypeus; width of face 0.7–0.8× height of eye and 1.2–1.3× height of face and clypeus combined. Diameter of antennal socket 1.3–1.5× distance between sockets. Clypeus 2.0–2.5× wider than its median height. Hypoclypeal depression as wide as distance from edge of depression to eye, 0.4–0.45× width of face.

Antennae slightly thickened, almost filiform, 25-segmented, as long as body. Scape 1.6–1.8× longer than maximum width (lateral view), 2.0× longer than pedicel. First flagellar segment 2.5–3.0× longer than apical width, as long as second segment. Penultimate segment 2.7–3.0× longer than width.

Mesosoma: long and high, its length 1.75–1.8× maximum height. Mesoscutum 1.2–1.3× as wide as its median length. Median lobe of mesoscutum slightly protruding anteriorly, distinctly convex on anterior margin. Notauli distinctly and densely crenulate, finely coriaceous between crenulae. Prescutellar sulcus (depression) finely coriaceous, with seven distinct carinae, 0.35–0.4× as long as scutellar disc. Metanotum (dorsal view) with distinct median and two convergent posteriorly lateral carinae, posterior convex area narrow. Sternaulus entirely finely and densely crenulate-reticulate or only reticulate, running along anterior 0.5–0.6 of lower part of mesopleuron.

Wings: forewing 2.9–3.0× longer than maximum width. Vein R1 (metacarp) 1.3–1.4× longer than pterostigma. Vein 3RSa (second radial abscissa) 1.5–1.6× longer than vein r (first abscissa), 0.3× as long as the almost straight vein 3RSb (third abscissa), 0.8× as long as vein 2RS (first radiomedial). Second radiomedial vein (vein r-m) slightly inclivous. Second submarginal (radiomedial) cell 2.6–2.8× longer than maximum width, about 1.3× longer than first subdiscal (brachial) cell. Vein RS + M (first medial abscissa) curved. Vein M + CU (mediocubital vein) slightly curved posteriorly. Distance from vein 1cu-a (nervulus) to vein 1M (basal) 0.8–1.0× vein 1cu-a (nervulus) length. Hindwing 4.8–5.0× longer than its maximum width. Vein M + CU (first abscissa of mediocubital vein) 0.6–0.8× as long as vein 1M (second abscissa) (until basal vein). Vein m-cu (recurrent vein) strongly desclerotised, interstitial.

Legs: Hind coxa 1.6–1.7× longer than wide (with basal angle). Hind femur 3.6–3.8× longer than wide. Hind tarsus almost as long as hind tibia. Hind tibia distinctly widened towards apex. Second segment of hind tarsus 0.5–0.6× as long as basitarsus, 1.2–1.3× longer than fifth segment (without pretarsus).

Metasoma: 1.1–1.2× longer than head and mesosoma combined. First tergite slightly convex (lateral view) and slightly-curvedly widened from base to apex (dorsal view), 1.7–1.75× longer than apical width, 1.55–1.6× longer than propodeum; maximum width of tergite about 2.0× its minimum width. Suture between second and third tergites mostly absent. Median length of second and third tergites combined 1.6–1.8× basal width of second tergite, about 0.7× maximum width of third tergite. Ovipositor sheaths 1.2–1.3× longer than metasoma, about 2.2× longer than mesosoma, about 0.9× as long as forewing.

Sculpture and pubescence: vertex, frons and face finely and densely granulate-coriaceous, temple finely coriaceous to smooth posteriorly. Mesoscutum entirely densely reticulate-coriaceous, almost smooth posteriorly, without

additional striation, striate with rugosity in a narrow area in medioposterior 0.3 of mesoscutum. Scutellar disc almost entirely smooth. Mesopleuron finely reticulate-coriaceous. Propodeum with areas distinctly delineated by carinae; basolateral areas medium size, entirely finely coriaceous, without rugosity along carinae; areola long and wide, connected anteriorly with base of propodeum (without basal carina), entirely coarsely rugose-reticulate; petiolate area short and transverse; propodeum in posterior half mostly smooth between rather sparse and distinct carinae. Hind coxa finely coriaceous. Hind femur reticulate-coriaceous. First metasomal tergite with coarse, and more or less regular longitudinal striae, with dense and distinct rugosity between striae. Second tergite striate with dense reticulation between striae in basal 0.6–0.8; third tergite distinctly striate subbasally. Remaining tergites smooth. Vertex densely setose, setae short and directed forwards. Mesoscutum with short and semi-erect setae situated in narrow lines along notauli and along edges. Hind tibia dorsally with long, sparse and semi-erect setae, length of setae 0.4–0.8× maximum width of hind tibia.

Colour: body brownish yellow to light reddish brown; propodeum, first and mediobasal half of second metasomal tergites dark brown to black; metapleuron reddish brown. Antennae dark brown to black, three to seven basal segments brownish yellow to pale brown. Palpi pale yellow. Legs yellow to brownish yellow, tarsal segments darker. Ovipositor sheaths pale brown or brown, dark brown to black in apical 0.3–0.4. Forewing subhyaline or very faintly infuscate. Pterostigma brown, pale brown to yellow marginally.

Male. Body length 2.6 mm; forewing length 1.8 mm. Head less transverse, its width 1.5× median length. Transverse diameter of eye 2.0× longer than temple. Penultimate segment 2.3× longer than their width. Vein 3RSa (second radial abscissa) 0.9× as long as vein 2RS (first radiomedial). Second submarginal (radiomedial) cell 3.0× longer than maximum width. Hindwing without stigma-like enlargement. Hindwing slightly widened, 3.2× longer than wide. First tergite 2.1× longer than apical width, 1.5× longer than propodeum; maximum width about 1.7× its minimum width. Third tergite indistinctly sculptured. Otherwise similar to female.

Distribution. Costa Rica.

Biology. The type specimens were reared from syconia of *Ficus hemsleyana* King.

Etymology. This species is named after the Costa Rican people, who call themselves 'ticos'.

Type material. Holotype: female (IB-UNAM), 'Costa Rica, La Guaria de Piedades, Sur de San Ramón Alajuela, 10°06′N–84°32′W, 950 msnm, 5.i.2008, *Ficus hemsleyana*, J. Vasquez'; DNA voucher no CNIN-1100, GenBank accession no. KJ586718 (*COI*), KJ586787 (*28S*), KJ586696 (*wg*), KJ586750 (*16S*).

Paratypes: one female, one male, same data as holotype (IB-UNAM).

Sabinita Belokobylskij, Zaldívar-Riverón et Martínez, gen.n.

http://zoobank.org/urn:lsid:zoobank.org:act:031DED59-09C3-40FD-AEB9-84F6C3C8F085
(Figs 4F, 9A–F)

Type-species. Sabinita mexicana **sp.n.**

Diagnosis. Species of *Sabinita* morphologically resemble those of *Allorhogas*, though they can be distinguished by having the basal sternal plate (acrosternite) of first metasomal segment distinctly elongated, 0.4–0.5× as long as the first tergite (0.25 or less in species of *Allorhogas*), scape of antenna with distinct ventroapical lobe and length of its ventral margin (lateral view) equal or longer than dorsal one (without ventroapical lobe and its ventral margin shorter than dorsal one in *Allorhogas*), and the hind coxa without distinct basoventral tubercle (always present in *Allorhogas*). *Sabinita* is also similar to *Psenobolus*, *Ficobolus* and *Plesiopsenobulus*, but they can be distinguished by the features mentioned in the key to genera (see below).

Description. Female. Small, 2.5–2.7 mm. *Head*: not depressed, transverse. Vertex densely granulate. Ocelli arranged in triangle with base 1.2–1.3× its sides. Frons with distinct and wide excavation running from lateral ocelli, with distinct, thick and not high median longitudinal keel, with lateral protuberances emarginated dorsally by distinct longitudinal carina. Eyes with sparse and short setae. Occipital carina complete, fused with hypostomal carina before mandibles. Malar suture absent. Clypeus high, delineated from face by a distinct furrow, with fine lower flange. Hypoclypeal depression small and rounded. Postgenal bridge wide. Maxillary palpi long, 6-segmented, apical segment about as long as fifth segment; labial palpi long, 4-segmented, third segment not shortened. Scape of antenna wide and short, with a flange apically and with a short ventroapical lobe, without basal constriction; ventral margin of scape as long as dorsal margin (lateral view). First flagellar segment subcylindrical, slightly curved, slightly longer than second segment. Apical segment pointed apically, without 'spine'.

Mesosoma: not depressed, short. Neck of prothorax short. Pronotum slightly convex dorsally (lateral view), with short anterior flange curved up; pronotal carina almost indistinct. Pronope absent. Propleural dorsoposterior flange long and wide. Mesonotum highly and almost perpendicularly elevated above pronotum, mostly granulate. Median lobe of mesonotum without median longitudinal furrow, anterolateral corner wide and obtuse. Notauli complete, deep, and wide. Tegula evenly widened distally, not concave along outer margin. Scuto-scutellar suture distinct and complete. Prescutellar sulcus (depression) long, with high carinae. Lateral longitudinal flanges on level of prescutellar depression low. Scutellar disc slightly convex, longer than wide, with lateral carinae. Subalar

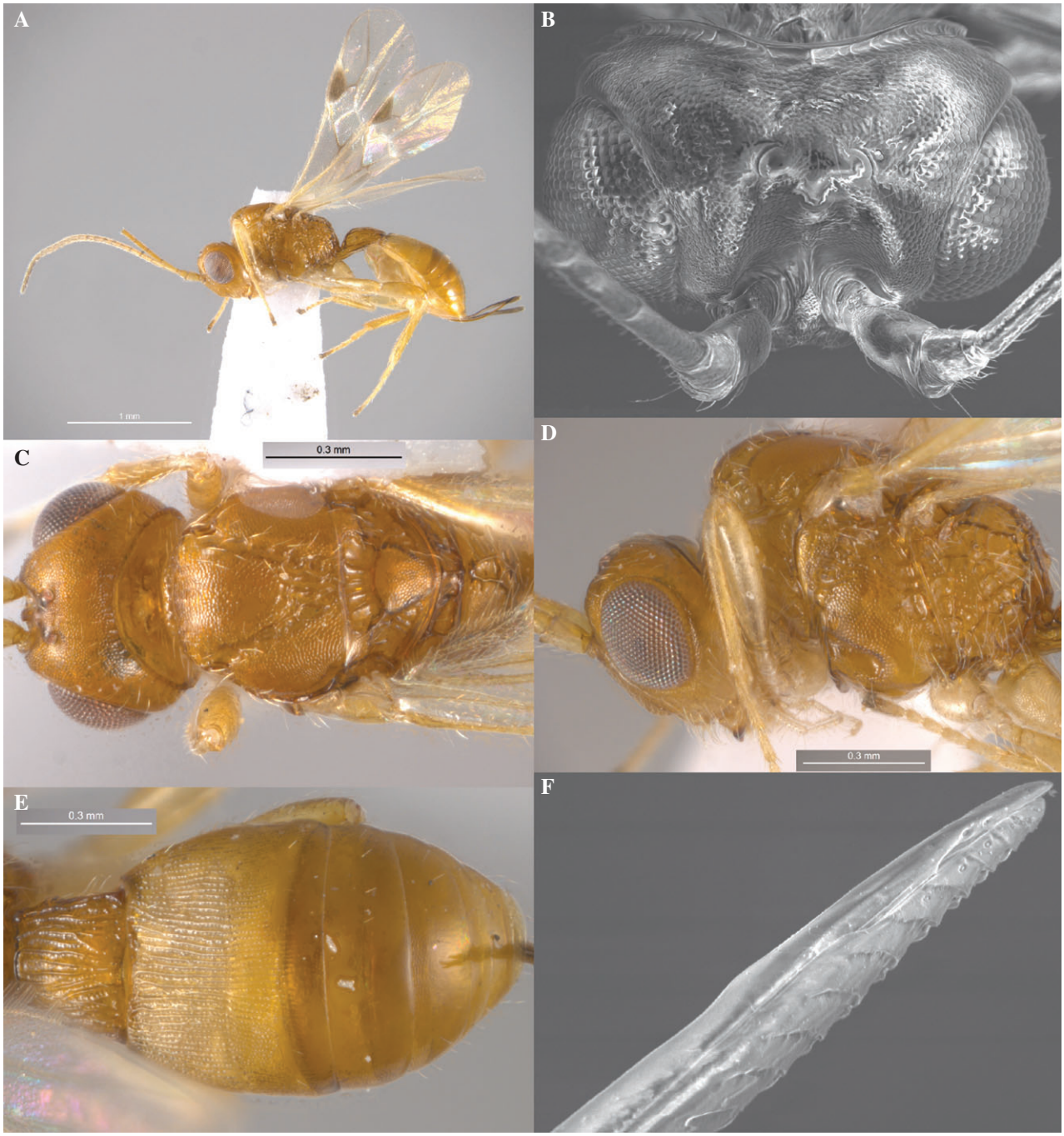

Fig. 9. *Sabinita mexicana* **sp.n.** Holotype, female: (A) habitus (lateral view); (B) head, scape and pedicel, dorsal view; (C) mesosoma and head (dorsal view); (D) mesosoma and head (lateral view); (E) metasoma (dorsal view); (F) ovipositor apex.

depression distinct and narrow. Mesopleural pit distinct. Sternaulus deep, wide, short, straight and oblique. Prepectal carina distinct and complete, high ventrally, laterally reaching lower margin of subalar depression. Postpectal carina absent. Metanotum without median tooth (lateral view). Metapleural flange long, rounded apically. Propodeum with areas delineated by distinct carinae; lateral tubercles present, distinct, short and wide; propodeal bridge absent. Propodeal spiracles small and rounded. Metapleuron slightly convex, entirely sculptured.

Wings: pterostigma of forewing wide and short. Vein r (first radial abscissa) arising from middle of pterostigma. Marginal (radial) cell slightly shortened. Veins 2RS and r-m (first and second radiomedial veins) present. Second submarginal (radiomedial) cell short and narrow. Vein 1m-cu (recurrent vein) usually

distinctly postfurcal. Vein 1cu-a (nervulus) distinctly postfurcal. First discal (discoidal) cell petiolate anteriorly, vein 1RS (petiole of discoidall cell) long. Veins 1M (basal) and 1m-cu (recurrent) subparallel. Vein 3CU (parallel vein) not interstitial, distinctly curved basally. First subdiscal (brachial) cell open postero-apically, vein 2cu-a (brachial vein) completely absent. Veins 1a and 2a (transverse anal veins) absent. Hindwing with three hamuli. Vein C + Sc + R (first abscissa of costal vein) 1.3–1.5× longer than vein SC + R (second abscissa). Vein RS (radial vein) arising from vein R (costal vein) far from vein r-m (basal vein). Marginal (radial) cell slightly widened basally, then distinctly narrowed towards apex, without vein r (transverse vein). Basal (medial) cell not widened from middle towards apex, 10.0–12.0× longer than width, 0.25–0.3× as long as hindwing. Vein cu-a (nervellus) present. Subbasal (submedial) cell long. Vein M + CU (first abscissa of mediocubital vein) about as long as vein M (second abscissa). Vein m-cu (recurrent vein) long, slightly oblique toward apex of wing, slightly curved.

Legs: inner surface of fore tibia with several long and slender spines arranged in a single vertical line. Fore tarsus 1.2–1.3× longer than fore tibia. Middle tibia with spines on anterior surface. Middle tarsal segments long. Hind coxa short and wide, with distinct basoventral angle and without distinct tubercle. Fore and middle femora without dorsal protuberances. Hind femur wide and elongate-oval. Hind tibia with a comb of dense setae along its inner distal margin. Basitarsus of hind tarsus 0.4–0.45× as long as second–fifth segments combined. Claws short and simple.

Metasoma: first tergite semi-petiolate, short, wide and distinctly convex. Basal sternal plate (acrosternite) distinctly elongate, 0.4–0.5× as long as first tergite, situated behind spiracular level. Dorsope small but distinct; basolateral lobes almost absent; spiracular tubercles distinct, spiracles situated in basal 0.4–0.5 of tergite. First tergite on basal fifth with a high and coarse semi-circular transverse carina, with distinct, subparallel and almost complete dorsal carinae. Second tergite without furrows and areas. Second suture shallow, complete, slightly sinuate. Third tergite with very shallow transverse submedian furrow separating a wide basal area. Second to sixth tergites with separate laterotergites. Third and remaining tergites with a single transverse line of sparse short erect setae. Posterior margin of hypopygium not narrowed and truncate apically. Ovipositor without distinct nodes. Ovipositor sheaths distinctly shorter than metasoma.

Biology. The only described species assigned to *Sabinita* were reared from leaf galls of an undescribed species of *Ficus* (see below).

Distribution. Neotropical region (Mexico).

Etymology. We named this genus after Sabina Zaldívar-Jacobo, AZR's daughter.

Remarks. In all our phylogenetic analyses, the sister taxon of *S. mexicana* **sp.n.** was a male also collected in Chamela, Mexico [DNA voucher number ASDOR 082; GenBank accession no. HM434332 (*COI*), HQ200621 (*28S*)]. Most of the external morphological features of this specimen are concordant with those of *Sabinita*, though it lacks the ventroapical lobe on the scape of antenna and the vein 1m-cu (recurrent) of the forewing is antefurcal.

Sabinita mexicana Belokobylskij, Zaldívar-Riverón et Martínez sp.n.

http://zoobank.org/urn:lsid:zoobank.org:act:56A3156B-CA17-499D-913E-F03B8F37537F
(Figs 4F, 9A–F)

Description. Female. Body length 2.52.7 mm; forewing length 1.8–2.0 mm. *Head*: width 1.5–1.7× median length, 1.05–1.15× width of mesoscutum. Head behind eyes (dorsal view) distinctly and almost linearly narrowed posteriorly. Transverse diameter of eye 2.5× longer than temple. Ocellar triangle situated almost on middle of head (dorsal view). Ocelli medium-sized, arranged in triangle with base 1.2–1.3× its sides. POL 1.1–1.2× Od, 0.3–0.5× OOL. Eye without emargination opposite antennal socket, 1.2× higher than broad. Malar space 0.4–0.45× height of eye, 1.0–1.1× basal width of mandible. Face with carinae along eyes, with shallow short depressions above clypeus; face width 0.9× height of eye and 0.9–1.0× height of face and clypeus combined. Diameter of antennal socket about equal to distance between sockets. Clypeus about as wide as its median height. Hypoclypeal depression 0.5–0.55× as wide as distance from edge of depression to eye, 0.3× face width.

Antennae slender, filiform, 23–24-segmented, about as long as body. Scape 1.7–1.8× longer than maximum width (lateral view), 2.0× longer than pedicel. First flagellar segment 4.0–4.5× longer than apical width, 1.0–1.1× long than second segment. Penultimate segment 2.0–2.3× longer than wide, 0.9× as long as apical segment.

Mesosoma: short and high, its length 1.4–1.5× maximum height. Mesoscutum 1.3–1.4× as wide as median length. Median lobe of mesoscutum slightly protruding anteriorly, almost straight on anterior margin. Notauli distinctly and sparsely crenulate, smooth or finely coriaceous between crenulae. Prescutellar sulcus (depression) finely granulate-coriaceous, partly smooth, with three to four coarse carinae, 0.45–0.5× as long as scutellar disc. Metanotum (dorsal view) with distinct median and two slightly posteriorly convergent lateral carinae, posterior convex area absent. Sternaulus finely and densely crenulate-granulate, running along anterior half of lower part of mesopleuron.

Wings: forewing 2.9–3.2× longer than maximum width. Vein R1 (metacarp) 1.2–1.3× longer than pterostigma. Vein 3RSa (second radial abscissa) 1.6–2.5× longer than vein r (first abscissa), 0.3–0.4× as long as slightly curved vein 3RSb (third abscissa), 0.7–1.0× as long as vein 2RS (first radiomedial). Second submarginal (radiomedial) cell 3.0–3.4× longer than maximum width, about 1.5× longer than first subdiscal (brachial) cell. Vein RS + M (first medial abscissa) distinctly

sinuate. Vein M + CU (mediocubital vein) slightly curved posteriorly. Distance from vein 1cu-a (nervulus) to vein 1M (basal vein) 0.6–0.8× vein 1cu-a (nervulus) length. Hindwing 4.0–4.3× longer than maximum width. Vein M + CU (first abscissa of mediocubital vein) about as long as vein 1M (second abscissa). Vein m-cu (recurrent) strongly unsclerotised, postfurcal.

Legs: hind coxa 1.4–1.5× longer than wide (with basal angle). Hind femur 3.5–3.8× longer than wide. Hind tarsus 0.8–0.9× as long as hind tibia. Second segment of hind tarsus 0.6–0.7× as long as basitarsus, 1.2–1.4× longer than fifth segment (without pretarsus).

Metasoma: 1.1–1.2× longer than head and mesosoma combined. First tergite strongly convex (lateral view), distinctly and almost linearly widened from base to apex (dorsal view), 1.0–1.1× longer than its apical width; maximum width of tergite 2.2–2.4× minimum width. Median length of second tergite 0.55–0.6× basal width, about 1.1× length of third tergite. Ovipositor sheath 0.4–0.5× as long as metasoma, 0.65–0.7× as long as mesosoma, 0.3× as long as forewing.

Sculpture and pubescence: vertex and face distinctly and densely granulate; frons (including cavity) and temple densely and finely granulate. Mesoscutum densely granulate, without striation, rugose-areolate in wide and short area in medio-posterior 0.25–0.30 of mesoscutum. Scutellar disc densely and sometimes finely granulate or granulate-coriaceous. Mesopleuron densely reticulate-coriaceous. Propodeum with areas distinctly delineated by carinae; basolateral areas short, semi-rounded, entirely granulate; areola long and narrow, connected anteriorly with base of propodeum (without basal carina), with a few coarse transverse carinae; petiolate area (if separated from areola by carina) long; posterior half of propodeum mostly smooth between carinae. Hind coxa transversally striate-granulate dorsally, remaining area granulate. Hind femur entirely reticulate-coriaceous. First tergite with coarse, sparse and curved striae, with dense and fine additional rugulosity between striae. Second and third tergites densely striate, striae becoming finer and transformed into fine and dense punctation in posterior 0.2–0.3 of third tergite, apical stripe of third tergite smooth. Fourth tergite in basal half and fifth tergite in basal third densely and finely punctate-reticulate, smooth apically. Remaining tergites smooth. Vertex densely and entirely setose, setae directed forwards. Mesoscutum with short, pale and semi-erect setae along notauli and edges. Hind tibia with short, rather dense and semi-erect setae dorsally, length of setae 0.3–0.5× maximum width of hind tibia.

Colour: body yellowish brown, metasoma medially yellow. Antennae yellow basally, darker in apical half. Palpi pale yellow. Legs entirely yellow, hind tibia paler basally. Ovipositor sheaths brown. Forewing faintly infuscate. Pterostigma brown, paler basally and apically.

Male. Unknown.

Distribution. Mexico.

Biology. The four known specimens of this species were reared from leaf galls on an unidentified species of *Ficus* at the beginning of the rainy season of 2012 in Chamela, Jalisco, Mexico. These galls contained a single specimen each, were rounded, small (less than 1 cm in diameter), indistinctly protruding and had a brownish coloration.

Type material. Holotype: female (IB-UNAM). 'Mexico, Jalisco, Est. Biol. Chamela, Camino Calandria, ex *Ficus*, reared 2.vii.2012, A. Zaldivar-Riveron col'; DNA voucher no. CNIN 1291; GenBank accession nos KJ586722 (*COI*), KJ586791 (*28S*).

Paratypes: three females (IB-UNAM, ZISP), same data as holotype.

Key to the gall-associated genera of Doryctinae

1. Vein r-m (second radiomedial) of forewing absent. Vein cu-a (nervulus) antefurcal. Vein M + CU (mediocubital) strongly curved on apical half. Vein (RS + M)b (second abscissa of medial) distinctly longer than veins m-cu (recurrent) and 2RS (first radiomedial). Forewing on dorsal side with large bare areas. Propodeal bridge present. Scutellar disc strongly convex. Reared from galls induced by other insects on Fabaceae (commonly associated with *Prosopis* species, the association with *Caesalpinia* needs to be confirmed) . . . . . *Percnobracon* Kieffer et Jorgensen
– Vein r-m (second radiomedial) of forewing present. Vein cu-a (nervulus) not antefurcal. Vein M + CU (mediocubital) not or slightly curved on apical half. Vein (RS + M)b (second abscissa of medial) not longer than veins m-cu (recurrent) and 2RS (first radiomedial). Forewing on dorsal side without bare areas. Propodeal bridge absent. Scutellar disc slightly convex 2

2. Vein 2RS (first radiomedial) of forewing strongly reduced or absent. Vein cu-a (nervellus) of hindwing absent, subbasal (submedial) cell widely open. Ovipositor shorter that first metasomal tergite. Probably gall-inducer, reared from aerial roots and leaves of *Ficus* species . . . . . *Labania* Hedqvist
– Vein 2RS (first radiomedial) always present. Vein cu-a (nervellus) of hindwing usually present (except for some specimens of *Mononeuron*), subbasal (submedial) cell usually closed. Ovipositor usually distinctly longer than first metasomal tergite 3

3. Vein 3Cu (parallel) of forewing interstitial or subinterstitial, not curved basally. Vein m-cu (recurrent) of hindwing distinctly curved towards base. Ovipositor not shorter than body. Prepectal carina usually absent or at least incomplete on wide lateral parts. Median mesosternal depression on lower part of mesosoma usually wide and deep. Recorded as gall-inducers on *Philodendron* and *Anthurium* species (Araceae) . . . . . *Monitoriella* Hedqvist
– Vein 3Cu (parallel) of forewing not interstitial, distinctly curved basally. Vein m-cu (recurrent) of hindwing not curved towards the base, usually subperpendicular to vein M (medial) or curved towards apex of wing. Ovipositor usually distinctly shorter than body. Prepectal carina always present and complete. Median mesosternal depression on lower part of mesosoma narrow and shallow 4

4. Basal sternal plate (acrosternite) of first metasomal segment not elongated, distinctly shorter than half of first metasomal tergite. First metasomal tergite usually short and wide. Hind coxa usually with a basoventral tubercle 5
– Basal sternal plate (acrosternite) of first metasomal segment distinctly or strongly elongated, equal to or longer than half of first metasomal tergite. First metasomal tergite usually long and narrow. Hind coxa without basoventral tubercle 6

5. Vertex at least partly striate. Veins SC + R (second abscissa of costal) and cu-a (nervellus) of hindwing almost absent or spectral. Ovipositor distinctly longer than metasoma. One described species, probably gall-inducer on leaves of *Duguetia furfurescea* (Annonaceae) . . . . . *Mononeuron* Fischer
– Vertex entirely granulate, sometimes with rugosities. Veins SC + R (second abscissa of costal) and cu-a (nervellus) of hindwing present and tubular. Ovipositor shorter to slightly longer than metasoma. Some species have been recorded as gall-inducers in fruits of three plant families, but others appear to be parasitoids/inquilines in galls induced by other insects . . . . . *Allorhogas* Gahan (also *Donquickeia* Marsh**;** see discussion section).

6. Prescutellar sulcus (depression) short, with numerous carinae (Fig. 4D). Scutellar disc wide, transverse, its maximum width about 1.3× its maximum length, 6.0–7.0× longer than prescutellar sulcus (Fig. 4D). Notauli narrow, always incomplete, reduced posteriorly and never connected with anterior margin of prescutellar sulcus (Fig. 4D). Propodeum always without areas and areola delineated by carinae, mainly smooth or only partly slightly sculptured (Fig. 4D). Hind coxa without basoventral corner. Apparently only associated with syconia of *Ficus* species (Fig. 1G) . . . . . *Psenobolus* Reinhard
– Prescutellar sulcus (depression) long, usually with sparse and a few carinae (Figs 5C, 6D, 7C, 8B, 9C). Scutellar disc subtriangular, its maximum width often equal to or less than its maximum length, 2.0–3.0× longer than prescutellar sulcus (Figs 5C, 6D, 7C, 8B, 9C). Notauli usually wide, always complete, not reduced posteriorly and always connected with anterior margin of prescutellar sulcus (Figs 5C, 6D, 7C, 8B, 9C). Propodeum always with areas and areola delineated by coarse carinae, mainly sculptured (Figs 5C, 6D, 7C, 8B, 9C). Hind coxa with basoventral corner. Mostly associated with galls on vegetative organs of *Ficus* species 7

7. First metasomal tergite short and wide (Fig. 9E); basal sternal plate (acrosternite) short, only 0.4–0.5× as long as first tergite. Scape of antenna with distinct ventroapical lobe (Fig. 9B); length of ventral margin of scape (lateral view) not less than length of its dorsal margin. 1m-cu (recurrent) vein of forewing distinctly postfurcal (Fig. 4F). Propodeum with distinct and subpointed lateral tubercles (Fig. 9D). Median keel of frontal cavity thick and obtuse dorsally (Fig. 9B) . . . . . *Sabinita* **gen.n.**
– First metasomal tergite long or rather long and more or less narrow (Figs 5A, 7D, 8D); basal sternal plate (acrosternite) long, 0.7–0.8× as long as first tergite. Scape of antenna without ventroapical lobe (Figs 5B, 6D, 8B); length of ventral margin of scape (lateral view) always less than length of its dorsal margin. 1m-cu (recurrent) vein of forewing antefurcal or sometimes almost interstitial, never postfurcal (Figs 4E, 7E, F). Propodeum without lateral tubercles, if present, short and subrounded (Figs 5E, 7B, 8C). Median keel of frontal cavity rather slender and more or less pointed dorsally (Figs 5D, 6B) 8

8. First flagellar segment long, distinctly longer than second segment (Fig. 5B). Frontal cavity laterally marginated almost completely by sharp longitudinal carina (Figs 5D, 6B). Median lobe of mesosonotum often with distinct median longitudinal furrow. Mesopleuron entirely coarsely rugose with granulation, always with additional and at least incomplete oblique furrow (Figs 5E, 6C). Sternaulus running to posterior margin of mesopleuron (Figs 5E, 6C). Metapleural flange short, wide in lateral and posterior views. Ovipositor sheaths distinctly shorter than metasoma (Figs 5A, 6A) . . . . . *Ficobolus* **gen.n.**
– First flagellar segment not long, about as long as second segment. Frontal cavity laterally without or with fine and incomplete longitudinal carina. Median lobe of mesosoma always without median longitudinal furrow. Mesopleuron entirely only granulate, without additional oblique furrow (Figs 7B, 8C). Sternaulus not running to posterior margin of mesopleuron (Figs 7B, 8C). Metapleural flange long, narrow in lateral and posterior views. Ovipositor sheaths longer than metasoma (Figs 7A, 8A) . . . . . *Plesiopsenobolus* **gen.n.**

Supporting Information

Additional Supporting Information may be found in the online version of this article under the DOI reference: 10.1111/syen.12078

Figure S1. Bayesian and ML phylograms reconstructed with five datasets containing different levels of missing taxa/characters. Black circles represent Bayesian posterior probabilities and bootstrap values ≥0.95 and ≥70, respectively; hollow circles represent Bayesian posterior probabilities and bootstrap values between 0.9–0.94 and 50–69, respectively.

Table S1. Records of gall-associated doryctine species and their host plant families previous to this study.

Table S2. List of specimens included in the phylogenetic analyses, their locality details and GenBank accession numbers for the four examined loci.

Table S3. Primers and PCR annealing conditions employed in this study for the four gene markers examined.

Table S4. Models of evolution selected in jModeltest for each partition examined in this study. PI = parsimony informative sites.

Table S5. Results obtained by the three tests of alternative topologies (stepping stone, Shimodaira-Hasegawa and Approximate Unbiased approaches) carried out in this study.

File S1. Nexus file containing the concatenated matrix with all examined taxa and sequences.

Acknowledgements

We thank Cristina Mayorga and Gabriela Aguilar for their help mounting the specimens examined in this study; Andrea Jiménez for her help in the laboratory; Federico Paniagua, Jefrey Vásquez and Hans Clebsh for their help in collecting some of the specimens; Rafael Torres and Guillermo Ibarra for identifying the *Ficus* species from Guerrero; and Susana Guzmán and Berenit Mendoza for their assistance taking the stereoscopic digital microscope and the SEM pictures at the Instituto de Biología, UNAM. This study was supported by grants given by CONACyT, Mexico (Red Temática del Código de Barras de la Vida) and PAPIIT (DGAPA-UNAM, convocatoria 2013) to AZR, a grant given by the Russian Foundation for Basic Research (No. 13-04-00026) to SAB, a grant given by ANPCyT' Argentina (PICT 2012′0617 Préstamo BID) to JJM, and by a postdoctoral fellowship given by DGAPA-UNAM (convocatoria 2012) to CPL. This research was also supported in part by National Science Foundation grants DEB-07-17034 and DEB-10-20751 (Caterpillars and parasitoids in the Eastern Andes of Ecuador, CAPEA) to SRS. Any opinions, findings, and conclusions expressed are those of the authors and do not necessarily reflect the views of the National Science Foundation.

References

van Achterberg, C. & Marsh, P.M. (2002) Revision of the genus *Psenobolus* Reinhard (Hymenoptera: Braconidae: Doryctinae). *Zoologische Mededelingen Leiden*, **76**, 1–25.

van Achterberg, C. & Weiblen, G.D. (2000) *Ficobracon brusi* gen.nov. & spec. nov. (Hymenoptera: Braconidae), a parasitoid reared from figs in Papua New Guinea. *Zoologische Mededelingen Leiden*, **74**, 51–55.

Belokobylskij, S.A. (1992) On the classification and phylogeny of the braconid wasp subfamilies Doryctinae and Exothecinae (Hymenoptera, Braconidae). Part I. On the classification. *Entomologicheskoe Obozrenie*, **71**, 900–928.

Belokobylskij, S.A. (2006) *Neoheterospilus* gen. n., a new genus of the tribe Heterospilini (Hymenoptera: Braconidae, Doryctinae) with highly modified ovipositor and a worldwide distribution. *Insect Systematics and Evolution*, **37**, 149–178.

Belokobylskij, S.A. & Tobias V.I. (1998). Fam. Braconidae. Introduction. *Key to Insects of the Russian Far East. Neuropteroidea, Mecoptera, Hymenoptera,* Vol. 4 (ed. by P.A Lehr), pp. 8–26. Dal'nauka, Vladivostok (in Russian).

Belshaw, R. & Quicke, D.L.J. (1997) A molecular phylogeny of the Aphidiinae (Hymenoptera: Braconidae). *Molecular Phylogenetics and Evolution*, **7**, 281–293.

Brèthes, J. (1922) Himenópteros y Dípteros de varias procedencias. *Anales de la Sociedad Científica Argentina*, **93**, 119–149.

Brower, A.V.Z. & DeSalle, R. (1998) Patterns of mitochondrial versus nuclear DNA sequence divergence among nymphalid butterflies: the utility of *wingless* as a source of characters for phylogenetic inference. *Insect Molecular Biology*, **7**, 73–82.

Ceccarelli, F.S. & Zaldívar-Riverón, A. (2013) Broad polyphyly and historical biogeography of the Neotropical wasp genus *Notiospathius* (Braconidae: Doryctinae). *Molecular Phylogenetics and Evolution*, **69**, 142–152.

Ceccarelli, F.S., Sharkey, M.J. & Zaldívar-Riverón, A. (2012) Species identification in the taxonomically neglected, highly diverse Neotropical parasitoid wasp genus *Notiospathius* (Braconidae: Doryctinae) based on an integrative molecular and morphological approach. *Molecular Phylogenetics and Evolution*, **62**, 485–495.

Centrella, M.L. & Shaw, S.R. (2010) A new species of phytophagous braconid *Allorhogas minimus* (Hymenoptera: Braconidae: Doryctinae) reared from fruit galls on *Miconia longifolia* (Melastomataceae) in Costa Rica. *International Journal of Tropical Insect Science*, **30**, 101–107.

Centrella, M.L. & Shaw, S.R. (2013) Three new species of gall-associated *Allorhogas* wasps from Costa Rica (Hymenoptera: Braconidae: Doryctinae). *International Journal of Tropical Insect Science*, **33**, 145–152.

Chavarría, L., Hanson, P., Marsh, P. & Shaw, S.R. (2009) A phytophagous braconid, *Allorhogas conostegia* sp. nov. (Hymenoptera: Braconidae), in the fruits of *Conostegia xalapensis* (Bonpl.) D. Don (Melastomataceae). *Journal of Natural History*, **43**, 2677–2689.

Cook, J.M., Rokas, A., Pagel, M. & Stone, G.N. (2002) Evolutionary shifts between host oak species and host plant organs in *Andricus* gall wasps. *Evolution*, **56**, 1821–1830.

Costa Lima, A.M. (1954) Um novo *Doryctes* da Colombia (Hymenoptera: Braconidae: Doryctinae). *Revista Brasileira de Entomologia*, **2**, 1–5.

Csóka, G., Stone, G.N. & Melika, G. (2005). Biology, ecology and evolution of gall-inducing Cynipidae. *Biology, Ecology, and Evolution of Gall-Inducing Arthropods* (ed. by A. Raman, W.C. Schaefer and T.M. Whiters), pp. 573–642. Science Publishers: Enfield, NH.

Dangerfield, P.C. & Austin, A.D. (1998) Biology of *Mesostoa kerri* (Insecta: Hymenoptera: Braconidae: Mesostoinae), an endemic Australian wasp that causes stem galls on *Banskia marginata*. *Australian Journal of Botany*, **46**, 559–569.

Doss, R.P, Oliver, J.E., Proebsting, W.M. *et al.* (2000). Bruchins: insect-derived plant regulators that simulate neoplasm formation. *Proceedings of the National Academy of Sciences of the United States of America*, **97**, 6218–6223.

Dowton, M. & Austin, A.D. (2001) Simultaneous analysis of 16S, 28S, COI and morphology in the Hymenoptera: Apocrita-evolutionary transitions among parasitic wasps. *Biological Journal of the Linnean Society*, **74**, 87–111.

Drummond, A.J., Suchard, M.A., Xie, D. & Rambaut, A. (2012) Bayesian phylogenetics with BEAUti and the BEAST 1.7. *Molecular Biology and Evolution*, **29**, 1969–1973.

Fischer, M. (1960) Revision der palaarktischen Arten der Gattung *Heterospilus* Haliday (Hymenoptera, Braconidae). *Polskie Pismo Entomologiczne*, **30**, 33–64.

Fischer, M. (1981) Versuch einer systematischen Gliederung der Doryctinae, insbesondere der Doryctini, und Redeskription nach material aus den Naturwissenschaftlichen Museum in Budapest (Hymenoptera: Braconidae). *Polskie Pismo Entomologiczne*, **51**, 41–99.

Flores, S., Nassar, J.M. & Quicke, D.L.J. (2005) Reproductive phenology and pre-dispersal seed predation in *Protium tovarense* (Burseraceae), with description of the first known phytophagous "*Bracon*" species (Hymenoptera: Braconidae: Braconinae). *Journal of Natural History*, **39**, 3663–3685.

Folmer, O., Black, M., Hoeh, W., Lutz, R. & Vrijenhoek, R. (1994) DNA primers for amplification of mithochondrial cytochrome *c* oxidase subunit I from diverse metazoan invertebrates. *Molecular Marine Biology and Biotechnology*, **3**, 294–299.

Gahan, A.B. (1912) Descriptions of two new genera and six new species of parasitic Hymenoptera. *Proceedings of the Entomological Society of Washington*, **14**, 2–8.

Harper, L.J., Schönrogge, K., Lim, K.Y., Francis, P. & Lichtenstein, C.P. (2004) Cynipd galls: insect-induced modifications of plant development create novel plant organs. *Plant, Cell and Environment*, **27**, 327–335.

Hartley, S.E. (1998) The chemical composition of plant galls: are levels of nutrients and secondary compounds controlled by the gall-former? *Oecologia*, **113**, 492–501.

Hasegawa, M., Kishino, H. & Yano, T. (1985) Dating of the human-ape splitting by a molecular clock of mitochondrial DNA. *Journal of Molecular Evolution*, **22**, 160–174.

Hedqvist, K.J. (1963) Notes on Hormiinae with description of new genera and species (Hym., Ichneumonoidea, Braconidae). *Entomologisk Tidskrift*, **84**, 30–61.

Infante, F., Hanson, P. & Wharton, R. (1995) Phytophagy in the genus *Monitoriella* (Hymenoptera: Braconidae) with description of new species. *Annals of the Entomological Society of America*, **88**, 406–415.

Jobb, G., von Haeseler, A. & Strimmer, K. (2004) TREEFINDER: a powerful graphical analysis environment for molecular phylogenetics. *BMC Evolutionary Biology*, **4**, 18.

Jukes, T.H. & Cantor, C.R. (1969). Evolution of protein molecules. *Mammalian Protein Metabolism* (ed. by H.N. Munro), pp. 21-132, Academic Press, New York, NY.

Kieffer, J.J. & Jörgensen, P. (1910) Gallen und Gallentiere aus Argentinien. *Centralblatt für Bakteriologie, Parasitenkunde und Infektionskrankheiten*, **27**, 362–442.

Kimura, M. (1980) A simple method for estimating evolutionary rates of base substitutions through comparative studies of nucleotide sequences. *Journal of Molecular Evolution*, **16**, 111–120.

Koyama, Y., Yao, I. & Akimoto, S.I. (2004) Aphid galls accumulate high concentrations of amino acids: a support for the nutrition hypothesis for gall formation. *Entomologia Experimentalis et Applicata*, **113**, 35–44.

Lanave, C.G., Preparata, C., Saccone, C. & Serio, G. (1984) A new method for calculating evolutionary substitution rates. *Journal of Molecular Evolution*, **20**, 86–93.

Larson, K.C. (1998) The impact of two gall-forming arthropods on the photosynthetic rates of their hosts. *Oecologia*, **115**, 161–166.

LaSalle, J. (2005). Biology of gall inducers and evolution of gall induction in Chalcidoidea (Hymenoptera: Eulophidae, Eurytomidae, Pteromalidae, Tanaostigmatidae, Torymidae). *Biology, Ecology, and Evolution of Gall-Inducing Arthropods* (ed. by A. Raman, W.C. Schaefer and T.M. Whiters), pp. 507–537, Science Publishers, Enfield, NH.

de Macêdo, M.V. & Monteiro, R.T. (1989) Seed predation by a braconid wasp, *Allorhogas* sp. (Hymenoptera). *Journal of the New York Entomological Society*, **97**, 359–362.

de Macêdo, M.V., Pimentel, M.C. & Vieira, R.C. (1998) Response of *Pithecellobium tortum* Martius (Leguminosae) seeds to the attack of the phytophagous braconid *Allorhogas dyspistus* Marsh (Hymenoptera: Braconidae). *Journal of Hymenoptera Research*, **7**, 274–279.

Maddison, D.R. & Maddison, W.P. (2000) *MacClade 4: Analysis of Phylogeny and Character Evolution*. Sinauer Associates, Sunderland, MA.

Marsh, P.M. (1991) Description of a phytophagous doryctine braconid from Brazil (Hymenoptera: Braconidae). *Proceedings of the Entomological Society of Washington*, **93**, 92–95.

Marsh, P.M. (1993) Descriptions of new Western Hemisphere genera of the subfamily Doryctinae (Hymenoptera: Braconidae). *Contributions of the American Entomological Institute*, **28**, 1–58.

Marsh, P.M. (1997a) Replacement names for Western Hemisphere genera of the subfamily Doryctinae (Hymenoptera: Braconidae). *Proceedings of the Entomological Society of Washington*, **99**, 586.

Marsh, P.M. (1997b). Subfamily Doryctinae. *Manual of the New World Genera of the Family Braconidae (Hymenoptera)*, Special Publication No. 1. (ed. by R.A. Wharton, P.M. Marsh and M.J. Sharkey), pp. 206–233. International Society of Hymenopterists, Washington, DC.

Marsh, P.M. (2002) The Doryctinae of Costa Rica (excluding the genus *Heterospilus*). *Memoirs of the American Entomological Institute*, **70**, 1–319.

Marsh, P.M., de Macêdo, M.V. & Pimentel, M.C. (2000) Description and biological notes on two new phytophagous species of the genus *Allorhogas* from Brazil (Hymenoptera: Braconidae: Doryctinae). *Journal of Hymenoptera Research*, **9**, 292–297.

Marsh, P.M., Wild, A.L. & Whitfield, J.B. (2013) The Doryctinae (Braconidae) of Costa Rica: genera and species of the tribe Heterospilini. *ZooKeys*, **347**, 1–474.

Martínez, J.J. (2006) Three new species of *Percnobracon* Kieffer & Jörgensen (Hymenoptera: Braconidae) from Argentina, reared from cecidomyiid (Diptera) and eurytomid (Hymenoptera) galls. *Zootaxa*, **1282**, 49–58.

Martínez, J.J. & Zaldívar-Riverón, A. (2013) Seven new species of *Allorhogas* (Hymenoptera: Braconidae: Doryctinae) from Mexico. *Revista Mexicana de Biodiversidad*, **84**, 117–139.

Martínez, J.J., Zaldivar-Riverón, A. & Sáez, A.G. (2008) Reclassification of *"Bracon" mendocinus* Kieffer & Jörgensen (Hymenoptera: Braconidae) a gall associated doryctine wasp, and description of a new closely related species of *Allorhogas*. *Journal of Natural History*, **42**, 2689–2701.

Martínez, J.J., Altamirano, A. & Salvo, A. (2011) New species of *Allorhogas* Gahan (Hymenoptera: Braconidae) reared from galls on *Lycium cestroides* Schltdl. (Solanaceae) in Argentina. *Entomological Science*, **14**, 304–308.

Miller, M.A., Pfeiffer, W. & Schwartz, T. (2010) Creating the CIPRES Science Gateway for inference of large phylogenetic trees. *Proceedings of the Gateway Computing Environments Workshop (GCE)*, pp. 1–8. IEEE, New Orleans, Louisiana.

Muesebeck, C.F.W. (1960) A fossil braconid wasp of the genus *Ecphylus* (Hymenoptera). *Journal of Paleontology*, **34**, 495–496.

Nunes, J.F., Penteado-Dias, A.M., Ceccarelli, F.S. & Zaldívar-Riverón, A. (2012) Redescription of *Mononeuron duguetiae* Fischer (Braconidae, Doryctinae), a gall associated species on *Duguetia furfuracea* (St. Hil.) (Annonnaceae). *Journal of Hymenoptera Research*, **24**, 75–84.

Nylander, J.A.A. (2004) *MrModeltest v.1.0b* [WWW document]. URL http://www.ebc.uu.se/systzoo/staff/nylander.html [accessed on 15 November 2013].

Nylander, J.A.A., Ronquist, F., Huelsenbeck, J.P. & Nieves-Aldrey, J.L. (2004) Bayesian phylogenetic analyses of combined data. *Systematic Biology*, **53**, 1–21.

Patankar, R., Sean, C. & Smith, S.M. (2011) A gall-inducing arthropod drives declines in canopy tree photosynthesis. *Oecologia*, **167**, 701–709.

Penteado-Dias, A.M. (2000). Biological notes and larval morphology of *Donquickeia* (Hymenoptera: Braconidae: Doryctinae). *Hymenoptera, Evolution, Biodiversity and Biological Control* (ed. by A.D. Austin and M. Wharton), pp. 296–299, SCIRO Publishing, Collingwood.

Penteado-Dias, A.M. & de Carvalho, F.M. (2008) New species of Hymenoptera associated with galls on *Calliandra brevipes* Benth. (Fabaceae, Mimosoidea) in Brazil. *Revista Brasileira de Entomologia*, **52**, 305–310.

Perioto, N.W., Lara, R.I.R, Ferrerira, C.S. *et al.*(2011). A new phytophagous *Bracon* Fabricius (Hymenoptera: Braconidae) associated with *Protium ovatum* (Burseraceae) fruits from Brazilian savannah. *Zootaxa*, **3000**, 59–65.

Quicke, D.L.J. (1997) *Parasitic Wasps*. Chapman & Hall, London.

Raman, A., Schaeffer, C.W. & Withers, T.M. (2005). Galls and gall inducing arthropods: an overview of their biology, ecology and evolution. *Biology, Ecology, and Evolution of Gall-inducing Arthropods* (ed. by A. Raman, W.C. Schaefer and T.M. Whiters), pp. 1–33, Science Publishers: Enfield, NH.

Ramírez, B.W. & Marsh, P.M. (1996) A review of the genus *Psenobolus* (Hymenoptera: Braconidae) from Costa Rica, an inquiline fig wasp with brachypterous males, with descriptions of two new species. *Journal of Hymenoptera Research*, **5**, 64–72.

Reinhard, H. (1885). *Psenobolus* nov. gen. *Feigeninsekten (Hymenoptera),* Vol. 35 (ed. by G. Mayr), pp. 246–247, 147–250. Verhandlungen der Zoologische-Botanische Gesellschaft Wien.

Roininen, H., Nyman, T. & Zinovjev, A. (2005). Biology, ecology, and evolution of gall-inducing sawflies (Hymenoptera: Tenthredinidae and Xyelidae). *Biology, Ecology, and Evolution of Gall-Inducing Arthropods* (ed. by A. Raman, W.C. Schaefer and T.M. Whiters), pp. 467–494. Science Publishers, Enfield, NH.

Ronquist, F. (1995) Phylogeny and early evolution of the Cynipoidea. *Systematic Entomology*, **20**, 309–335.

Ronquist, F., Teslenko, M., van der Mark, P. *et al.* (2012). MrBayes 3.2: efficient Bayesian phylogenetic inference and model choice across large model space. *Systematic Biology*, **61**, 539–542.

Sharkey, S.R., Wharton, R.A. (1997). Morphology and terminology. *Manual of the New World Genera of the Familiy Braconidae (Hymenoptera)*, *Special Publication of the International Society of Hymenopterists*, Vol. 1 (ed. by R.A. Wharton, P.M. Marsh and M.J. Sharkey), 19–37. The International Society of Hymenopterists, Washington, District of Columbia.

Shenefelt, R.D. & Marsh, P.M. (1976) *Hymenopterorum Catalogus*, Pars 13. Braconidae 9. Doryctinae. Dr W. Junk, 's-Gravenhage.

Shimbori, E.M., Penteado-Dias, A.M. & Nunes, J.F. (2011) *Monitoriella* Hedqvist (Hymenoptera: Braconidae: Doryctinae) from Brazil, with descriptions of three new species. *Zootaxa*, **2921**, 28–38.

Shimodaira, H. (2002) An approximately unbiased test of phylogenetic tree selection. *Systematic Biology*, **51**, 492–508.

Shimodaira, H. & Hasegawa, M. (1999) Multiple comparisons of log-likelihoods with applications to phylogenetic inference. *Molecular Biology and Evolution*, **16**, 1114–1116.

Stamatakis, A., Hoover, P. & Rougemont, J. (2008) A rapid bootstrap algorithm for the RAxML Web Servers. *Systematic Biology*, **57**, 758–771.

Taeger, A., Blank, S.M. & Liston, A.D. (2010) World catalog of Symphyta (Hymenoptera). *Zootaxa*, **2580**, 1–1064.

Wei, P., Li, Z., van Achterberg, C., Feng, G., Xiao, H. & Huang, D.W. (2013) Two new species of the genus *Ficobracon* van Achterberg and Weiblen (Hymenoptera: Braconidae) from China, expanding its host range. *Zootaxa*, **3640**, 465–472.

Wharton, R.A. & Hanson, P.E. (2005). Gall wasps in the family Braconidae (Hymenoptera). *Biology, Ecology, and Evolution of Gall-inducing Arthropods* (ed. by A. Raman, W.C. Schaefer and T.M. Whiters), pp. 495–505, Science Publishers, Enfield, NH.

Woodburne, M.O. & Case, J.A. (1996) Dispersal, vicariance, and the late Cretaceous to early Tertiary land mammal biogeography from South America to Australia. *Journal of Mammalian Evolution*, **3**, 121–161.

Xie, W., Lewis, P.O., Fan, Y., Kuo, L. & Chen, M.H. (2011) Improving marginal likelihood estimation for Bayesian phylogenetic model selection. *Systematic Biology*, **60**, 150–160.

Zaldívar-Riverón, A., Mori, M. & Quicke, D.L.J. (2006) Systematics of the cyclostome subfamilies of braconid parasitic wasps (Hymenoptera: Ichneumonoidea): a simultaneous molecular and morphological Bayesian approach. *Molecular Phylogenetics and Evolution*, **38**, 130–145.

Zaldívar-Riverón, A., Belokobylskij, S.A., Leon-Regagnon, V., Martínez, J.J., Briceño, R. & Quicke, D.L.J. (2007) A single origin of gall association in a group of parasitic wasps with disparate morphologies. *Molecular Phylogenetics and Evolution*, **44**, 981–992.

Zaldívar-Riverón, A., Belokobylskij, S.A., Leon-Regagnon, V., Briceño, R. & Quicke, D.L.J. (2008) Molecular phylogeny and historical biogeography of the cosmopolitan parasitic wasp subfamily Doryctinae (Hymenoptera : Braconidae). *Invertebrate Systematics*, **22**, 345–363.

Zuparko, R.L. & Poinar, G.O. Jr. (1997) *Aivalykus dominicanus* (Hymenoptera: Braconidae), a new species from Dominican amber. *Proceedings of the Entomological Society of Washington*, **99**, 744–747.

Accepted 25 March 2014